

Guideline for the assessment of MOSH/MOAH migration from packaging into food with the aim of minimization



Central organization
of the food industry

B|L

This guideline was developed within the scope of the IGF project "Measurement and prediction of the migration of mineral oil components (MOH) from packaging into food as a contribution to minimizing contamination" (AiF 19016 N) under the sponsorship of The Research Association of the Food Industry (FEI), which was funded by the Federal Ministry of Economic Affairs and Energy on the basis of a resolution of the German Bundestag.



Authors:

Ludwig Gruber
Romy Fengler
Dr. Roland Franz
Dr. Frank Welle
Prof. Dr. Heiko Briesen
Dr.-Ing. Christoph Kirse
Philip Schmid

Fraunhofer Institute for Process Engineering and Packaging IVV
Chair of Process Systems Engineering, Technical University of Munich

with the participation of the following members of the working group "Guideline" of the Project Monitoring Committee (PMC) of the AiF project AiF 19016 N:

Dr. Sieglinde Stähle
(PMC Chair)
Prof. Dr. Reinhard Matissek
(PMC Chair)
Dr. Stephan Baumgärtel
Markus Brunnbauer
Dr. Anne-Marie Calder
Henri Kamphuis
Dr. Hans-Michael Lenz
Dr. Hermann Onusseit
Christa Schuster-Salas
Dr. Michael Trenker
Claudia Wehmeier
Dr. Michael Winkler

German Federation of Food Law and Food Science (Bll e.V),
10117 Berlin, Germany
Institute of Food Chemistry (LCI) of the Federal Association of
the German Confectionery Industry, 51063 Cologne, Germany
Lubricants Industry Association, 20097 Hamburg, Germany
Backaldrin Österreich GmbH, 4481 Asten, Austria
August Storck KG, 33790 Halle (Westf.), Germany
Cargill b. v., Amsterdam, The Netherlands
ACTEGA Terra GmbH, 31275 Lehrte, Germany
Industrial Association for Food Technology and Packaging,
85354 Freising, Germany
Info point – Cocoa and more, 72760 Reutlingen, Germany
Mayr-Melnhof Karton GmbH, 8130 Frohnleiten, Austria
Treofan Germany GmbH, 66539 Neunkirchen, Germany
Association of the German Petroleum Industry, 10117 Berlin,
Germany

Publisher:

German Federation for Food Law and Food Science (BLL)
Claire-Waldoff-Straße 7
10117 Berlin

All rights reserved.

No part of this publication may be reprinted, translated or photographically reproduced, either in whole or in parts, without the permission of BLL.

Art work:

Sebastian Schuber, lieblingsgrafiker.de, Berlin, Germany

2. edition, February 2019

Table of contents

1.	Introduction	5
2.	Purpose and scope of application	6
3.	Initial concentration in packaging and food	8
4.	Calculation of migration via total mass transfer	9
5.	Calculation based on the assumption of equilibrium	10
5.1	Estimation of the partition coefficient	10
5.1.1	Direct food contact with paper	10
5.1.2	Paper packaging with indirect contact	11
5.2	Calculation formulas	12
6.	Consideration of contact conditions (t, T) and barrier characteristics of the packaging application	15
6.1	Type of contact with food	15
6.2	Functional barrier	16
6.2.1	Absolute functional barrier	16
6.2.2	Sufficient functional barrier	17
7.	Migration test and migration modelling	19
7.1	Migration tests of packaging/food combinations	19
7.2	Migration modelling	20
8.	Summary	22
9.	References	23
Annex		
A1.	Analysis of MOSH and MOAH	25
A2.	Evaluation methods for functional barriers	32
A3.	Migration test with food simulants	41
A4.	Determination of partition coefficient $K_{p,f}$	44
A5.	Numerical modelling of migrations	45
A6.	Disclaimer	49

List of abbreviations

BfR	Federal Institute for Risk Assessment, Germany
C ₁₈	Alkane with carbon chain length 18 (analogously also used for other chain lengths)
DIPN	Diisopropylnaphthalene; derived from carbonless copy paper; an indicator substance for recycled paper
FB	Functional barrier
FEM	Finite Element Method
FID	Flame ionization detector; carbon sensitive gas chromatography detector
GC-MS	Gas chromatography/mass spectrometry
HORRAT value	Statistical value for evaluating an interlaboratory comparison test; quotient of standard deviation and target standard deviation (estimated according to Horwitz); ideally, the values should be around 1
ILC	international interlaboratory comparison test
K _{p,f}	Partition coefficient between packaging (p) and food (f)
LC-GC	Liquid chromatography/gas chromatography coupling
MOAH	Mineral Oil Aromatic Hydrocarbons: hydrocarbons mainly consisting of highly alkylated mono- and/or poly-aromatic rings
MOH	Mineral Oil Hydrocarbons: generic term for MOSH and MOAH
MOSH	Mineral Oil Saturated Hydrocarbons: paraffin-like, open-chained, commonly branched hydrocarbons (e.g. alkanes) and naphthene-like cyclic hydrocarbons (cycloalkanes)
PA	Polyamide; polymer
PAO	Poly alpha olefins; component of synthetic lubricants and various hot melt adhesives. They can migrate into food and are difficult to distinguish analytically from MOSH
PE	Polyethylene; polymer
PET	Polyethylene terephthalate; polymer
POSH	Polymer Oligomeric Saturated Hydrocarbons: oligomers of the plastics polyethylene or polypropylene, which are chemically similar to MOSH and cannot be separated analytically
Δc _f	Change in concentration in the food due to migration from the packaging

1. Introduction

Mineral oil components from paper and other packaging materials and their migration into food have increasingly moved into the focus of consumer health protection agencies and food monitoring authorities.

With regard to the question of how the transfer of mineral oil components from cardboard packaging to foodstuffs can be minimized, the Federal Institute for Risk Assessment (BfR) refers to influencing factors such as the concentration in the packaging material, storage conditions and the type of food itself: Migration "can be prevented by using virgin fibre-based cardboard and mineral oil-free printing inks as well as by incorporating functional barriers in the design of the packaging. In this respect, it is not only the direct food packaging that must be taken into consideration but also the possibility of transfer from the outer packaging.." (BfR, 2012).

It is known that inner packagings made of paper or polyolefins on the one hand can delay migration (lag time) but cannot prevent it. However, films made of polyethylene terephthalate (PET) or polyamide (PA), on the other hand, are regarded as sufficiently migration-proof barriers that can effectively reduce or completely prevent the migration of mineral oil hydrocarbons (MOH) which comprise mineral oil saturated hydrocarbons (MOSH) as well as mineral oil aromatic hydrocarbons (MOAH) (Ewender et al. 2013). In any case, tight seals and undamaged films are assumed.

The successful reduction or prevention of contamination of a packaged food is a complex process (see also BLL Toolbox of December 2017), in which both the specific product sensitivities and the criteria for the packaging materials and solutions to be used must be taken into account. This applies not only to the finished product itself, but also to the raw materials and intermediate products used. These guidelines are intended to provide support, particularly for the packaging side.

2. Purpose and scope of application

The purpose of these guidelines is, on the one hand, to support companies in assessing packaging solutions already in use regarding their food law compliance in terms of mineral oil components. On the other hand, the document is intended to provide answers to the question of whether and if so, which measures are recommended or necessary to minimize or prevent MOH product exposure through other/alternative packaging solutions (barrier layers, inner bags, adsorber solutions or virgin fibre packaging). The answers to these questions must be considered in combination with the "BLL Toolbox for Preventing the Transfer of Undesired Mineral Oil Hydrocarbons into Food" (BLL, 2017) and the qualitative measures described therein. On this basis, the document focuses on understanding migration from packaging materials and quantitative criteria. These guidelines describe not only the basic migration principles but also a step-by-step procedure for checking and effectively developing a packaging/food combination. The key questions to ask include:

- How can the basic contamination of raw materials and packaging components be assessed? Are measurements required for that? (>> see Chapter 3)
- How can the worst-case of migration into the food be calculated under the assumption of total migration? (>> see Chapter 4)
- How can the migration into food be calculated under the assumption of equilibrium? Which measurements and/or data are required for that? (>> see Chapter 5)
- How can the migration be calculated under consideration of the physical nature of the material transfer (direct contact or transfer into the gas phase)? What types of measurements are required for that? (>> see Chapter 6)
- How can an inner liner or other barriers be assessed? What data already exists or what measurements (permeation measurements) are required? (>> see Annex)
- How can an advanced "Migration Modelling" be carried out? (>> see Chapter 7)

The following flow chart shows the principle of the step-by-step procedure. The underlying prediction models developed here represent new, alternative tools for quality assurance tests in the field of MOH.

Please note: For plastic packaging, such a model-based assessment has already been included in European legislation in 2001 (6th amendment of the European Plastics Directive 90/128/EEC).

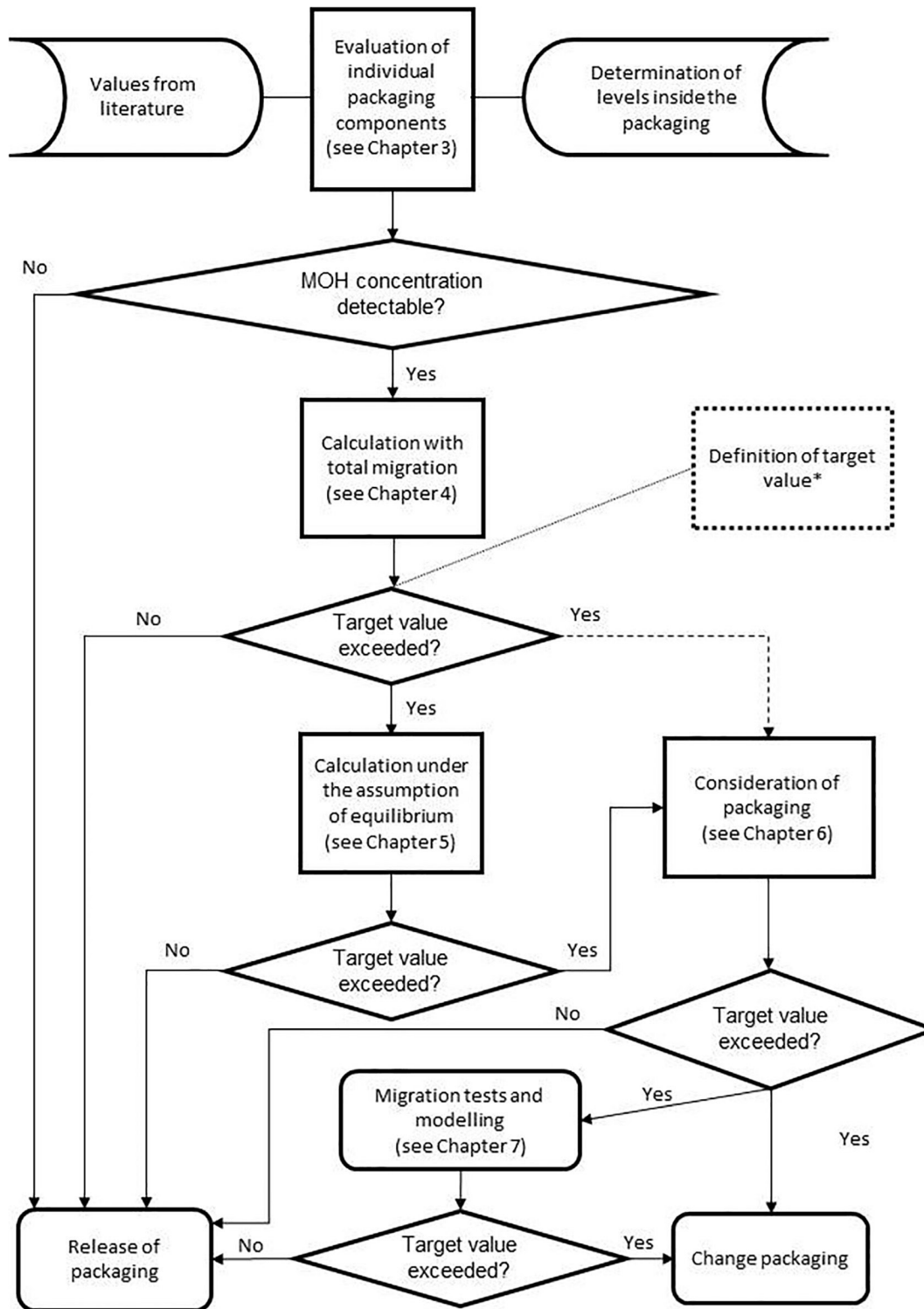


Figure 1: Flow chart used for assessing a packaging solution

* Target values must be defined by the user under consideration of legal requirements, possible customer specifications and voluntary commitments of the company.

3. Initial concentration in packaging and food

The first step when considering a possible mineral oil migration is to determine the initial concentration in the packaging material as well as determining the level already present in the food and in any preliminary products before packaging. If it can be ruled out that the packaging is a source of MOH, the packaging can be accepted without further action. In all other cases, at least a calculation based on total mass transfer (see Chapter 4) must be carried out in order to determine the possible influence of the packaging material on the MOH level in the food. If this does not bring about clear results, follow the flow chart.

In the following, the principle as well as the limits and issues to be considered in analytics are briefly explained. A detailed description with regards to analytics is included in the Annex. There are several methods available for the analysis of food and packaging. The reference method (BfR and Cantonal Laboratory Zurich (ed.), 2012) is LC-GC coupling, consisting of a system of liquid chromatography coupled to gas chromatography with FI detector. This method was developed by the Cantonal Laboratory Zurich. This routine method, which is currently commonly applied, does not allow to directly differentiate analytically between introduced MOSH, MOSH analogues (from mineral oil products such as paraffin), POSH (from plastics or adhesive applications) or partially detected native saturated hydrocarbons. This also applies analogously to the solid phase extraction method and GC-FID ("manual method"), published by BfR and Cantonal Laboratory Zurich (ed.), in 2012. In July 2017, a standardized European procedure (DIN EN 16955: 2017-08) for quantification in certain foods was published on the basis of LC-GC coupling. The method has been confirmed in ring tests; it is suitable for MOSH and MOAH levels from 10 mg/kg each in food based on vegetable fats. As recommended in the standard, the fossil origin of the MOSH and MOAH fractions should be verified by mass spectrometry (GC-MS or GCxGC-MS) if necessary.

For the so-called FABES method (Hauder et al., 2012) the percentage of substances with aromatic structures are determined by GC-MS from the total content of components that are able to migrate. The total content of MOH is determined by GC-FID. This requires an experienced laboratory, as the lack of liquid chromatographic pre-separation makes the manual detection of compounds necessary that are not MOAH, e.g. printing ink components containing aromatics (such as benzophenone derivatives), and the corresponding consideration in the evaluation.

In order to predict the migration as precisely as possible, the result of the analysis should include an indication of the different fractions in relation to the retention times of the n-alkanes, irrespective of the analytical method used. According to BfR (2012), for example, the following integration intervals are used, which allow at least a rough description of the mineral oil hump:

- $C_{10} - C_{16} / C_{16} - C_{20} / C_{20} - C_{25} / C_{25} - C_{35}$
- $C_{16} - C_{25}$ (sum of substances that are mobile via the gas phase)
- $C_{16} - C_{35}$ (sum of all substances that are able to migrate)

Further details and recommendations as to what should be included in the test report are provided in the Annex. Moreover, a "simplified method for the description of the mineral oil hump" is described, which allows a comparatively exact modelling of the migration behaviour.

4. Berechnung der Migration mit Totalübergang

The simplest estimation is based on the assumption that 100% of the MOSH or MOAH present in the packaging migrate into the packaged food (worst-case estimation). The calculation is carried out according to equation (1):

$$\Delta c_f = c_{p,0} \cdot \frac{m_p}{m_f} \quad (1)$$

Δc_f is the packaging-related increase in the concentration of MOSH or MOAH in food, calculated from the initial concentration of MOSH or MOAH in the packaging ($c_{p,0}$) and the masses of packaging (m_p) and packaged food (m_f).

If the value determined is less than the target value, the packaging can be released. The target value has to be determined on an individual basis.

According to equation (2), the concentration in food (c_f) is composed of the sum of the migration from the packaging Δc_f (migration) and the initial concentration in food ($c_{f,0}$):

$$c_f = \Delta c_f + c_{f,0} \quad (2)$$

If the value determined in this way is higher than the target value, it is recommended that a calculation based on the assumption of equilibrium (see Chapter 5) is used as the next step. If the target value is still exceeded in this step, or if this step is skipped, detailed consideration of the packaging application in question (see Chapter 6) is included in the next step.

Example 1:

For pasta (spiral noodles) packed in cardboard boxes, a measurement result of the packaging box is available. The initial concentration in the food $C_{f,0}$ equals 0. The MOSH level (C_{16} to C_{25}) in the cardboard corresponds to 10 mg/kg. The MOSH level (C_{25} to C_{35}) in the cardboard corresponds to 40 mg/kg. 500 g of the pasta is packed in 25 g of cardboard (8 dm², thickness $l = 500 \mu\text{m}$, density $d = 0.625 \text{ g/cm}^3$).

For the total mass transfer, the initial concentration in the C_{16} to C_{35} range must be used.

$$\Delta c_f = (10 + 40) \frac{\text{mg}}{\text{kg}} \cdot \frac{25 \text{ g}}{500 \text{ g}} = 2.5 \frac{\text{mg}}{\text{kg}} \text{ MOSH}$$

The calculation (according to equation 1) with the assumption of total mass transfer results in a maximum migration value and thus a maximum additional concentration in the food of 2.5 mg/kg MOSH.

5. Calculation based on the equilibrium assumption

The calculation of the migration under the equilibrium assumption is a less conservative, but usually, still a strict assumption that the equilibrium state is achieved in the distribution of MOH in the „packaged food“ system. If the value determined in this way is below the target value, the packaging can be released. If the value determined in this way is higher than the target value, the next assessment step under consideration of the packaging used shall be applied (see Chapter 6).

5.1 Estimation of the partition coefficient

To calculate the migration, the MOH partition coefficient between product and packaging must be known or available via a conservative estimation procedure (see Table 1). The MOH distribution varies in dependence of the volatility of the MOH as well as of the polarity and sorption capacity of both media, the carton/paper packaging and filled product.

In general, partition coefficient $K_{p,f}$ is defined as the ratio of the concentration of a migrant between the packaging (p) and the food (f) at the point when the state of equilibrium (∞) has been reached:

$$K_{p,f} = \frac{c_{p,\infty}}{c_{f,\infty}} \quad (3)$$

with $c_{p,\infty}$ or $c_{f,\infty}$ being the equilibrium concentrations of the migrant for the packaging or the food.

The fact that the partition coefficient is largely constant within the usual temperature range for food packagings (10°C to 60°C) is helpful for further evaluation (Seiler & Franz, 2012).

5.1.1 Direct food contact with paper

It is obvious that paper packaging is not suitable for all foods, and only for dry, fat-free and solid foods. Examples for direct contact with the paper include free-flowing salt, rice, noodles, flour and similar foods. In principle, such packaging systems can be depicted by a two-phase model:

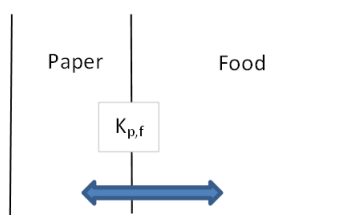


Figure 2: Two-phase model

Table 1 shows a list of $K_{p,f}$ values for paper determined for selected food. The foods are also representative of other, similar foods to which the corresponding $K_{p,f}$ value can be applied for orientation. The foods in the list with their different fat levels illustrate the different solubility or sorption characteristics of MOHs.

5.1.2 Paper packaging with indirect contact

Paper packaging with appropriate coatings, e.g. to achieve the necessary wet strength or with inner bags, is used for contact with any food. Such packaging systems can, in principle, be represented by a multiphase model with at least three phases:

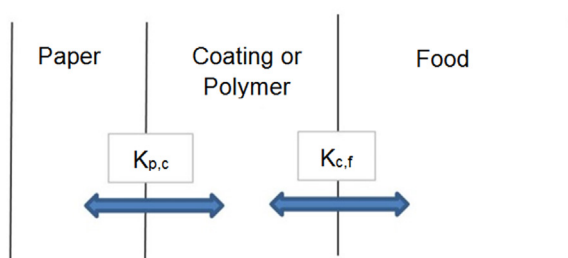


Figure 3: Three-phase model

For pragmatic reasons, in the absence of available measured data, a $K_{p,f}$ value between 1,000 for low solubility and 1 for high solubility in food is assumed for migration models in the field of plastic packaging. Based on systematic research within the EU projects FOODMIGROSURE and FACET, foods were classified by their similarity in solubility behaviour for chemical migrants. For packaging papers, $K_{p,f}$ values between 1,000 and 1 are assumed to be in line with the values measured in the FEI project (see Table 1); however, only for those foods that are suitable for paper packaging (also as secondary packaging).

Within the scope of the previous FACET project, investigations were also carried out on the distribution of model substances between paper and cardboard samples and LDPE film material. As a result, a value of 2 between paper and an overlying polyolefin layer was assumed in a first approximation as the general worst-case partition coefficient $K_{LDPE,paper}$. This K value can then be used to perform equilibrium assessments on multi-layer systems with the aid of migration modelling software, as shown in Figure 3 above. The classification of foods into groups was borrowed from the FACET project according to their equivalence to the solubility behaviour of ethanol-water mixtures.

Additional experiments in the underlying FEI project on partition coefficients between paper packaging and foods have been combined with the results of the previous FACET project (see Table 1) in such a way that these partition coefficients $K_{p,f}$ can be used computationally for an orienting evaluation of the migration. For simplification, the same density for food and packaging are assumed in the table.

For a more reliable calculation of the equilibrium state, an experimental determination of the $K_{p,f}$ values is recommended due to the variability of food types (see Annex).

Table 1: $K_{p,f}$ values for LDPE (or polyolefins in general) and paper used for estimations

Food	Packaging example	LDPE-ethanol-equiv. [%]	$K_{LDPE,f}$	$K_{paper,f}$ for MOSH experimental	$K_{paper,f}$ for MOAH experimental	$K_{paper,f}$
Crystallized sugar	Paper bag	0	1000	1000	1000	1000
Honey	PE screw closure with cardboard insert	0	1000	1000	1000	1000
Salt	Cardboard box	0	1000	400	400	500
Icing sugar	Cardboard box	0	500	45	70	50
Wine	Bag in Box	20	1000	no exp.	no exp.	1000
Tomato sauce	Bag in Box	25	1000	no exp.	no exp.	500
Noodles (without eggs)	Cardboard box or Bag in Box	35	1000	70	200	100
Wheat flour	Paper bag	35	500	no exp.	no exp.	50
Noodles (with eggs)	Cardboard box or Bag in Box	35	100	8	16	10
Rice	Cardboard box or Bag in Box	45	50	5	7	5
Fish fingers	Cardboard box (frozen)	40	50	no exp.	no exp.	5
Butter toast bread	Karton als Sekundärverpackung	50	50	no exp.	no exp.	5
Milk powder	Cardboard box or Bag in Box	50	50	no exp.	no exp.	5
Marzipan	Cardboard box as secondary packaging	60	50	6	8	5
Biscuits	Cardboard box	70	50	no exp.	no exp.	5
Chopped nuts	Cardboard box as secondary packaging	60	10	1	2	1
Ground nuts	Cardboard box as secondary packaging	60	1	no exp.	no exp.	1
Milk chocolate	Cardboard box as secondary packaging	95	1	1	2	1
Dark chocolate	Cardboard box as secondary packaging	95	1	no exp.	no exp.	1

no exp. = experimental data not yet available, therefore an estimation

5.2 Calculation formulas

If the partition coefficient is known, it is possible to calculate the increase in MOSH and MOAH levels in the equilibrium state (Δc_p) that is caused by the influence of the packaging.

To simplify things and because the respective MOSH and MOAH components have very similar polarity properties, it can be assumed that the partition coefficient for MOSH and MOAH is independent of the

molecule size. The packaging related migration achieved in the equilibrium is calculated according to equation (4)

$$\Delta c_f = \frac{\frac{m_p}{m_f}}{1 + \frac{m_p}{m_f} \cdot K_{p,f}} \cdot c_{p,0} \quad (4)$$

with the initial MOSH or MOAH concentrations in the packaging ($c_{p,0}$), as well as the masses of the packaging (m_p) and the packaged food in contact with the packaging (m_f).

The total concentration in the food results from equation (2).

For packaging in which there is an additional layer (usually a polymer layer) between the contaminated (paper) layer and the food, the increase in concentration is calculated according to equation (5).

$$\Delta c_f = \frac{\sum \frac{m_i}{m_f} \cdot (c_{i,0} - K_{i,f} \cdot c_{f,0})}{1 + \sum \frac{m_i}{m_f} \cdot K_{i,f}} \quad (5)$$

The equations overestimate the increase because equilibration happens in both directions and the initial concentration in the food is neglected.

Example 2a:

For pasta (spiral noodles without eggs) packed in cardboard boxes, a measurement result of the packaging box is available. The MOSH level (C_{16} to C_{25}) in the cardboard corresponds to 10 mg/kg. The MOSH level (C_{25} to C_{35}) in the cardboard corresponds to 40 mg/kg. 500 g of the pasta is packed in 25 g of cardboard (8 dm², thickness $l = 500 \mu\text{m}$, density $d = 0.625 \text{ g/cm}^3$).

In the range C_{16} to C_{35} the initial concentration must be used. The value in the table for paper and noodles (without egg in this case) is $K_{paper,f} = 100$. According to equation (4):

$$\Delta c_f = \frac{\frac{25 \text{ g}}{500 \text{ g}}}{1 + \frac{25 \text{ g}}{500 \text{ g}} \cdot 10} \cdot (10 + 40) \frac{\text{mg}}{\text{kg}} = 1.67 \frac{\text{mg}}{\text{kg}}$$

The calculation with assumption of the equilibrium distribution therefore provides a maximum migration value and thus a maximum additional concentration in the food of 0.42 mg/kg MOSH. This means, under consideration of the partition coefficient, there is less contamination of the food than calculated in example 1 for the total mass transfer.

Example 2b:

For example 2b, noodles are replaced by the same mass of milk chocolate.

Thus inserting a $K_{paper,f}$ value of 1 into equation (4) results in a Δc_f of 2.31 mg/kg. There is only a marginal calculated difference between the equilibrium related migration and the total mass transfer (example 1).

Example 3a:

Calculation example 2 is now expanded by the use of an LDPE layer as an inner coating or inner bag. The two-phase system turns into a three-phase system with the LDPE layer being in contact with the noodles (without eggs).

The partition coefficients used for noodles without eggs are:

$$K_{LDPE,f} = 1000 \text{ und } K_{p,f} = 100$$

The initial concentration in the range $C_{16} - C_{35}$ of 50 mg/kg must be used, because with an LDPE layer thickness of 10 μm , an LDPE density of 0.925 g/cm³ and the same LDPE area as the paper area, the LDPE mass is 0.74 g. According to equation (5) the migration is:

$$\Delta C_f = \frac{\frac{25\text{g}}{500\text{g}}}{1 + \frac{25\text{g}}{500\text{g}} \cdot 10 + \frac{0.74\text{g}}{500\text{g}} \cdot 1000} \cdot (10 + 40) \frac{\text{mg}}{\text{kg}} = 0.84 \frac{\text{mg}}{\text{kg}}$$

The calculation with assumption of the equilibrium distribution therefore provides a maximum migration value and thus a maximum increase in the concentration in the food of 0.334 mg/kg MOSH, which is a slight reduction compared to direct contact.

To illustrate the effect that the LDPE layer has on the MOSH concentration in food, different LDPE layer thicknesses from 10 μm to 300 μm were modelled for pasta and milk chocolate (Tables 2 and 3).

Table 2: Overview of MOSH concentrations (in mg/kg) after equilibration in each layer of the 3-phase system paper/LDPE/noodles as a function of LDPE layer thickness

Thickness of LDPE-Layer [μm]	MOSH [mg/kg]		
	Paper (500 μm)	LDPE	Noodles
10	38	255	0.334
30	29	196	0.239
50	24	159	0.186
100	16	108	0.120
300	7	47	0.050

The modelling shows that a polyolefin layer such as LDPE in contact with non-greasy, dry foods can act as a sorption trap for MOSH. However, the possible migration of POSH from the polyolefin itself is not taken into account here.

Example 3b:

When packaging a fatty food such as milk chocolate, the following situation would arise as shown in Table 3:

The partition coefficients inserted are: $K_{LDPE,f} = 1$ and $K_{paper,f} = 1$.

Table 3: Overview of MOSH concentrations (in mg/kg) after equilibration in each layer of the 3-phase system paper/LDPE/milk chocolate as a function of LDPE layer thickness

Thickness of LDPE-Layer [μm]	MOSH [mg/kg]		
	Paper (500 μm)	LDPE	Milk chocolate
10	3.70	2.50	2.31
30	3.69	2.49	2.30
50	3.68	2.48	2.30
100	3.65	2.47	2.28
300	3.55	2.40	2.22

The modelling of the equilibration shows that a polyolefin layer, regardless of its thickness, does not have any significant 'protective effect' when fatty foods are packaged. The MOSH concentrations determined in the chocolate are close to the total mass transfer (calculation example 1) and the equilibrium-related migration without PO layer (calculation example 2b).

6. Consideration of contact conditions (t,T) and barrier characteristics of the packaging application

If the target value is exceeded in both the total mass transfer and the equilibrium assumptions, the migration kinetics should be considered based on the filling and storage conditions of the specific packaging application. This is particularly important and effective when kinetic effects such as very slow diffusion through a packaging layer reduce or even prevent migration into the food, i.e. where functional barriers are used.

Polyolefins are not effective as diffusion barriers, however when they are used for non-greasy foods they can minimize MOH migration into the food via equilibrium (thermodynamic) or with only very short contact times (kinetic).

However, polymer layers with low diffusion, such as PET, can be effective kinetic functional barriers under common filling and storage conditions. Another important aspect here is the type of food contact, which is decisive for the qualitative composition of the migrating MOH. If necessary, defects in the packaging, such as pores or voids in sealed seams, as well as design errors such as perforation and folding must also be taken into consideration.

6.1 Type of contact with food

The type of contact between food and packaging affects the type of migration processes. In the case of direct (wetting) contact, it can be assumed as a rule of thumb that diffusion of molecules with chain lengths of C_{35} and more can largely be neglected.

During the transfer via the gas phase (typical in particular for dry food) MOSH and MOAH evaporate and precipitate on the food. This requires sufficient steam pressure. As a rule of thumb, it can be assumed that with chain lengths of up to C_{25} migration will take place at room temperature.

Migration from the packaging into the food is competing with evaporation to the outside. Experience has shown that compounds in the $<C_{16}$ range are hardly ever present in food due to their high volatility and can generally be neglected. Higher migration values in the $<C_{16}$ range are only to be expected for boxes placed or shrink-wrapped in shipping boxes. However, these cases have been sufficiently considered in the assumption that 100% of the mineral oil present in the packaging migrates into the product (worst-case estimation) or in the equilibrium assumption.

For the initial concentration in the packaging, the concentration in the range C_{10}/C_{16} to C_{25} is to be used for the simplified calculation models for transfer via the gas phase; for direct (wetting) contact, the concentration in the range C_{10}/C_{16} to C_{35} needs to be applied.

Example 4a:

For pasta (spiral noodles) packed in cardboard boxes, a measurement result of the packaging box is available. The MOSH level (C_{16} to C_{25}) in the cardboard corresponds to 10 mg/kg. The MOSH level (C_{25} to C_{35}) in the cardboard corresponds to 40 mg/kg. 500 g of the pasta is packed in 25 g of cardboard (8 dm², thickness $l = 500 \mu\text{m}$, density $d = 0.625 \text{ g/cm}^3$).

Since there is no complete surface-to-surface (wetting) contact between the packaging and the pasta and therefore transport via the gas phase can be assumed, the initial concentration range of $C_{16} - C_{25}$ can be used.

$$\Delta c_f = 10 \frac{\text{mg}}{\text{kg}} \cdot \frac{25\text{g}}{500\text{g}} = 0.5 \frac{\text{mg}}{\text{kg}} \text{ MOSH}$$

The calculation with assumption of total mass transfer results in a maximum migration value and thus a maximum additional concentration in the food of 2.5 mg/kg MOSH. This is clearly less than in example 1.

A further consideration takes into account the resulting equilibrium as in example 2a with $K_{\text{paper},f} = 100$. According to equation (4):

$$\Delta c_f = \frac{\left(\frac{25\text{g}}{500\text{g}}\right)}{1 + \frac{25\text{g}}{500\text{g}} \cdot 100} \cdot 10 \frac{\text{mg}}{\text{kg}} = 0.33 \frac{\text{mg}}{\text{kg}} \text{ MOSH}$$

The calculation with an assumption of the equilibrium distribution and a physically reasonable migration therefore provides a maximum migration value and thus a maximum additional concentration in the food of 0.083 mg/kg MOSH.

Example 4b:

If noodles as a product are replaced by milk chocolate, surface-to-surface contact must be assumed. The migration values from example 1 with 2.5 mg/kg and example 2b with 2.31 mg/kg do not change.

6.2 Functional barrier

"A functional barrier is a multi-layer packaging structure in which one layer prevents or delays the mass transfer process of a migrating substance through the packaging into the food." The requirement is considered to be approximately fulfilled if

$$t_b > t_{\text{shelf life food}}$$

with t_b being equal to the lag time (Ewender et al., 2016).

6.2.1 Absolute functional barrier

According to Art. 14 of Regulation (EU) No 10/2011, absolute functional barriers include:

- glass in any thickness, except with SiOx coating
- metal cans and closures
- aluminium films and coatings of a sufficient thickness so as to prevent pinholes or other damage (generally at least 6 µm thickness)

Studies show that polymers such as PET or OPA (barrier polymers) are also sufficient barriers. Annex A2 contains a list of *absolute functional barriers* and an overview of calculated "safe" polymer thicknesses.

6.2.2 Sufficient functional barrier

Polyolefins are not complete (absolute) functional barriers. Figure 4 shows relative barrier factors of different polymer barrier layers based on a HDPE film with 44 µm thickness. (Source: Fraunhofer IVV)

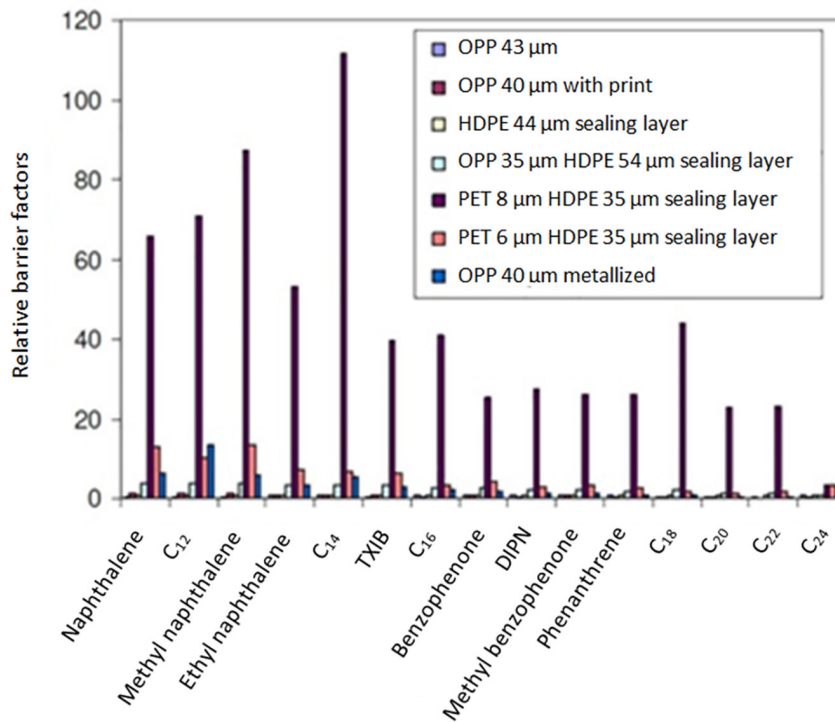


Figure 4: Relative barrier factors of different barrier layers (based on HDPE 44 µm)

A simple method for the evaluation of a functional barrier is based on experimentally determined permeation rates; it uses reference values or limits of quantification established by convention, e.g. 2 mg/kg MOSH or 0.5 mg/kg MOAH in food. With this method it is simply assumed that permeation takes place from the first minute with a constant permeation rate (no lag time). This results in an overestimation of permeation. If the permeation rate for a permeant and a barrier is known, the time until reaching e.g. the specific migration limit t_{SML} can be calculated according to equation 6. Here again, the evaluation applies only to the test conditions applied.

$$t_{SML} = \frac{SML \cdot m_f}{P \cdot A} \quad (6)$$

t_{SML} : Time until the SML has been reached (in days)

SML: Target value (specific migration limit in mg/kg food)

m_f : Mass of the food (in kg)

P: Permeation rate (experimentally determined in mg/(d dm²))

A: Area of contact of the packaging material (in dm²)

For less conservative considerations, please refer to the Annex. It should be taken into consideration that possible pores, micro holes and pinholes in barrier layers and physical processing (e.g. folding) can have a strong effect on the permeation behaviour of MOSH and MOAH. Examples for the presence of defects can be found in aluminium-coated BOPP (Langowski, 2008) or coated papers (Guazotti et al., 2015).

Example 5:

A food product is wrapped in paper equipped with a polyethylene coating with a thickness of 20 μm . The packaging is a cube with a surface area of 1 dm^2 on each side. The MOSH target value could be 0.5 mg/kg for example. The minimum shelf life of the product is 50 days. The density of the food is 1 kg/l . The permeation rate was determined by experiment; for the respective initial MOAH concentration, it is 88 $\text{mg}/\text{d dm}^2$ for DIPN.

The area of contact of the packaging material is $6 \times 1 \text{ dm}^2$. The weight of the food product is 1 kg . The time until the SML is reached is calculated according to equation 6:

$$t_{SML} = 0.5 \frac{\text{mg}}{\text{kg}} \cdot 1 \text{ kg} \cdot \left(0.088 \frac{\text{mg}}{\text{d dm}^2} \cdot 6 \text{ dm}^2 \right)^{-1} = 0.95 \text{ d} \approx \text{ca. 1 day}$$

The result (according to equation 6) shows clearly that e.g. polyethylene with a thickness of 20 μm is not a real (working) barrier.

7. Migration test and migration modelling

7.1 Migration tests of packaging/food combinations

For meaningful MOSH and MOAH migration tests, it is mandatory to select realistic conditions; this requires precise knowledge of the migration mechanisms.

It should be taken into consideration that MOSH and MOAH can migrate into the food, via the gas phase and via the solid phase. Tenax® and SorbStar® are two suitable simulants for the tests. SorbStar® is recommended for particulate food where Tenax® is able to excellently simulate fatty baked goods with a large internal surface.

For evaluating storage at room temperature for up to 12 months, storage tests for 10 days at 40°C are meaningful. For an intended storage period of 24 months, storage tests for 30 days at 40°C are recommended. Test temperatures above 40°C for further acceleration of the process have been proven unsuitable for respective migration tests (Castle, 2014).

The use of model substances (see Annex) for the simulation of mineral oil migration in spiked foods facilitates the evaluation, because the limits of quantification for individual substances are significantly lower and furthermore, it is more likely that concentrations already present in the food will not cause false results.

The following illustration shows a practical example for migration tests with noodles packed in a cardboard box.

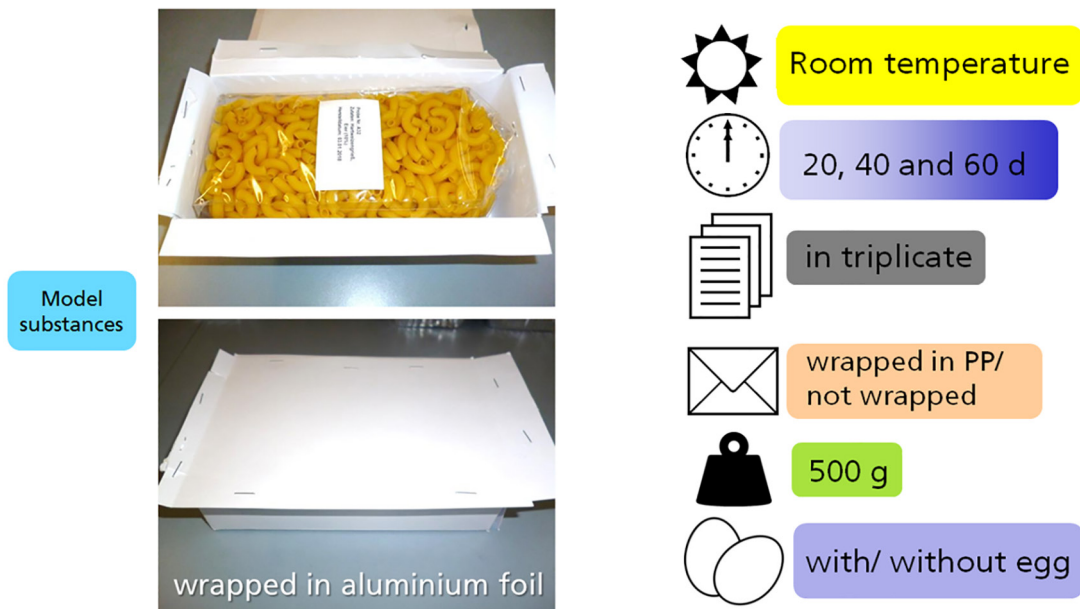


Figure 5: Practical example for migration tests of packaging/food combinations

7.2 Migration modelling

If the values determined by the calculation of migration with total mass transfer or the calculation under assumption of equilibrium are not sufficient for an evaluation of the packaging, it is possible to use numerical migration modelling which was introduced as a new, alternative tool for quality assurance tests for plastic packaging in European legislation in 2001. This method is highly complex for MOSH and MOAH and will therefore normally have to be carried out by test laboratories or research institutes.

Information about the packaging structure and the migration characteristics of the individual packaging layers is required for the migration modelling process. It is assumed that the migration of mineral oil components follows Fick's laws of diffusion. On the basis of these laws, a system of partial differential equations is formed, which tries to depict the migration process in terms of time and regions. Important information for a precise simulation concerns the diffusion coefficients of the mineral oil components through different packaging materials and foods. Equally important are the partition coefficients between packaging layers and the food.

The diffusion through such a characterized system can then be simulated. If the results of the simulation can be validated by experiments, then a tool has been created with which different packaging options can be predictively tested thus reducing the number of time-consuming migration tests.

Figure 6 shows an overview of the methods introduced so far for estimating the MOH concentration in food. In the example, the worst-case migration calculation according to equation (1) for the model substance C_{25} with total mass transfer results in a maximum value of 2.05 mg/kg. The calculation of the equilibrium assumption with a $K_{p,f}$ of 10 (see Table 1 for pasta with egg) results in a migrated amount of 1.34 mg/kg according to equation (4). The total mass transfer approach is the simplest form of estimation and leads to high, but often unrealistic values for the migration of MOHs. The equilibrium concentration is based on the thermodynamic equilibrium of the migration process and represents the possible final state of the migration. This value is always below the total mass transfer value, but can come very close to it, depending on the food. Both procedures depict the migration process without considering the time. The results of the migration modelling, plotted here for 20, 40 and 60 days, provide a more detailed picture of the migration process and show a lot of agreement with the experimental migration tests of the system investigated. This approach also shows that the equilibrium concentration has not yet been reached after 60 days.

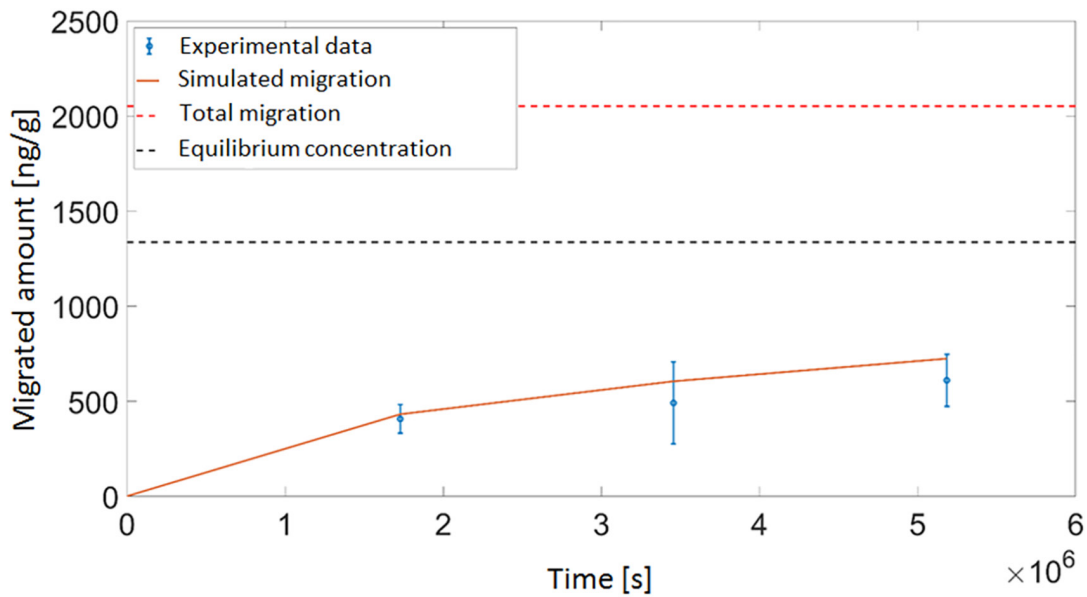


Figure 6: Comparison of results of migration tests for C₂₅ with the corresponding modelling

Performing an accurate migration simulation is highly demanding on experimental analytics and modelers and requires an exact characterization of the existing system. Nevertheless, it is a useful tool for the detailed analysis of migration as a function of the combination of packaging and food.

For simulating the migration of mixtures such as MOSH and MOAH, it is essential to indicate the shape of the mineral oil hump in the source. The mineral oil hump should be described as set out in the Annex. Indicating the concentrations of the individual fractions and the "simplified method for the description of the mineral oil hump" are sufficiently precise descriptions of the mineral oil hump; the description can be used in simplified calculation models for migration estimation. When comparing the exact calculation from the original data using the "simplified method" with data taken from chromatograms, the deviations are clearly below 10%. Therefore, the "simplified method" can also be applied retrospectively for measurements for which, for example, only printed chromatograms and total values are available.

8. Summary

Simplified calculation models can be used as a first approximation to estimate migration from the packaging into the food product. These methods are based on the assumptions of total mass transfer and thermodynamic equilibrium. For barriers, simplified considerations can be made based on permeation rates and calculated „safe“ thicknesses. Numerical migration modelling can, if necessary, describe the migration processes even more precisely.

The LC-GC measuring methods available for the determination of MOSH and MOAH in food and packaging are in general sufficient, but extended reporting requirements have to be fulfilled for the evaluation of possible migration by means of modelling. Indicating the concentrations of the individual fractions and the use of the mentioned „simplified method for the description of the mineral oil hump“ are sufficiently precise to describe the mineral oil hump; the description can be used in simplified calculation models for migration estimation.

For analytical reasons as well as for improved evaluation results, functional barriers should be studied with model substances. Permeation measuring systems offer some benefits:

- Automated measuring technology (at least one measuring point per day)
- Parallel determination of several films with simultaneous measurement of several (model) substances
- Accelerated tests (e.g. at 40°C) are possible
- Realistic approach (contaminated cardboard as a source)

For meaningful MOSH and MOAH migration tests, selecting realistic conditions is mandatory; this in turn requires precise knowledge of the migration mechanisms. It should be taken into consideration that both migration via the gas phase in the headspace of the packaging as well as direct contact migration by direct contact of the solid phases are possible.

9. Reference

- 6. Amendment of the European Plastics Regulation 90/128/EEC
- Becker, E., 2014. Mineralölkohlenwasserstoffe - Laborvergleichsstudie zu deren Bestimmung in Lebensmitteln und Verpackungsmaterialien. Deutsche Lebensmittel-Rundschau 3, 128-135
- BfR und Kantonales Labor Zürich (Hrsg.), 2012. Messung von Mineralöl – Kohlenwasserstoffen in Lebensmitteln und Verpackungsmaterialien. Bundesinstitut für Risikobewertung, Berlin
- BfR, 2012. Determination of hydrocarbons from mineral oil (MOSH & MOAH) or plastics (POSH & PAO) in packaging materials and dry foodstuffs by solid phase extraction and GC-FID, Berlin, 2012
- BLL, 2017. TOOLBOX BLL for Preventing the Transfer of Undesired Mineral Oil Hydrocarbons into Food. Berlin. Download under <https://www.bll.de/download/toolbox-for-preventing-the-transfer-of-undesired-mineral-oil-hydrocarbons-into-food>
- BMELV, 2012. Abschlussbericht zur wissenschaftlichen Studie „Ausmaß der Migration unerwünschter Stoffe aus Verpackungsmaterialien aus Altpapier in Lebensmittel“
- BMEL, 2017. Entwurf der „Mineralölverordnung“ – 22. VO zur Änderung der BedarfsgegenständeVO: 4. Entwurf vom 7. März 2017
- Brandsch, J., Mercea, P., Rüter, M., Tosa, V., Piringer, O., 2002. Migration modelling as a tool for quality assurance of food packaging. Food Additives and Contaminants 19, 29-41. doi:10.1080/02652030110058197
- Castle, L., 2015. Systematic derivation of Correction Factors (CFs) to relate chemical migration levels from paper and board into foods, with the migration or extraction values obtained using food simulants or solvents. CEPI
- Carson, J. K., Lovatt, S. J., Tanner, D. J., Cleland, A. C. 2005. Thermal conductivity bounds for isotropic, porous materials. International Journal of Heat and Mass Transfer, 48, 2150-2158. doi:10.1016/j.ijheatmasstransfer.2004.12.032
- Crank, J., 1975. The Mathematics of Diffusion: 2d Ed. Clarendon Press.
- DIN EN 16995:2017-08. Lebensmittel – Pflanzliche Öle und Lebensmittel auf Basis pflanzlicher Öle – Bestimmung von gesättigten Mineralöl-Kohlenwasserstoffen (MOSH) und aromatischen Mineralöl-Kohlenwasserstoffen (MOAH) mit online HPLC-GC-FID
- DIN SPEC 5010:2018-05. Testing of paper and board - Determination of the transfer of mineral oil hydrocarbons from food contact materials manufactured with portions of recycled pulp
- EFSA, 2012. Scientific opinion on mineral oil hydrocarbons in food, European Food Safety Authority
- Ewender, J., Fengler, R., Franz, R., Gruber, L., Welle, F., 2016. Funktionelle Barrieren gegen Mineralöl aus Papier- und Kartonverpackungen. DLG-Expertenwissen 10/2016. Download of the German-language version under https://www.dlg.org/fileadmin/downloads/food/Expertenwissen/Lebensmitteltechnologie/2016_10_Expertenwissen_Barrieren.pdf
- Ewender, J., Franz, R., Welle, F., 2013. Permeation of Mineral Oil Components from Cardboard Packaging Materials through Polymer Films. Packaging Technology and Science 26, 423-434
- Ewender, J., Langowski, H-C., Welle, F., 2015. Functional barriers towards mineral oil contaminants – Evaluation of alternatives to PET and PA. Verpackungs-Rundschau, Technisch-wissenschaftliche Beilage, pp. 50-51

- Flavourings, Additives and Food Contact Materials Exposure Task (FACET), 7th Framework EU funded project, 2008 to 2012, contract number: KBBE- 211686. <http://www.ucd.ie/facet/>
- Guazzotti, V., Limbo, S., Piergiovanni, L., Fengler, R., Fiedler, D., Gruber, L., 2015. A study into the potential barrier properties against mineral oils of starch-based coatings on paperboard for food packaging. *Food Packaging and Shelf Life* 3, 10
- Hauder, J., Benz, H., Rüter, M., Piringer, O., 2012. Experimentelle Bestimmung der Migration von Mineralölkomponenten aus Recyclingkarton in Lebensmittel Deutsche Lebensmittel-Rundschau 108, 135-142
- Joint Industry Group on Packaging for Food Contact (JIG) of the Swiss Packaging Institute SVI : SVI Guideline 2015.01_Innenbeutel, 2016
- Langowski, H.-C., 2008. Permeation of Gases and Condensable Substances through Monolayer and Multilayer Structures in Plastic Packaging. *Plastic Packaging: Interactions with Food and Pharmaceuticals*, Wiley-VCH, 2008
- Oldring, P.K.T., O'Mahony, C., Dixon, J., Vints, M., Mehegan, J., Dequatre, C., Castle, L., 2014 Development of a new modelling tool (FACET) to assess exposure to chemical migrants from food packaging. *Food Additives & Contaminants: Part A*, 31, 444-465. doi:10.1080/19440049.2013.862348
- Renaud, T., Briery, P., Andrieu, J., & Laurent, M. (1992). Thermal Properties of Model Foods in the Frozen State. *Journal of Food Engineering*, 15, 83-97. doi:10.1016/0260-8774(92)90027-4
- SciCom (Wetenschappelijk Comité van het Federaal Agentschap voor de Veiligheid van de Voedselketen – FAVV), 2017. Advies 19-2017 „Actiedrempels voor minerale olie koolwater stoffen in levensmiddelen”
- Van Den Houwe, K., Evrard, C., Van Loco, J., Lynen F., Van Hoeck, E., 2017. Use of Tenax® films to demonstrate the migration of chemical contaminants from cardboard into dry food. *Food Additives & Contaminants: Part A*, Volume 34, (7), p. 1261-1269. doi: 10.1080/19440049.2017.1326067
- Zurfluh, M., Biedermann, M., Grob, K., 2013. Simulation of the migration of mineral oil from recycled paperboard into dry foods by Tenax®? *Food Additives & Contaminants: Part A*, Vol. 30, pp. 909-918

Annex

A1 Analysis of MOSH and MOAH by means of LC-GC

The current reference method for MOSH and MOAH analysis is online LC-GC coupling.

A1.1 Achievable reproducibility

Table A1 below shows the reproducibility RSD_R , the resulting HORRAT values and extended measurement uncertainties U achieved in an international interlaboratory comparison test (ILC) (Becker, 2014).

Table A1: Reproducibility RSD_R achieved in an interlaboratory comparison test (Becker, 2014)

Matrix	MOSH RSD_R	Horrat	U (k=2)	MOAH RSD_R	Horrat	U (k=2)
Chocolate	39 %	3.5	80 %	34 %	2.5	70 %
Recycled cardboard	15 %	2.2	30 %	19 %	2.3	40 %
Rice	20 %	1.4	40 %	39 %	2.1	80 %
Hazelnut oil	31 %	3.0	60 %	50 %	4.0	100 %

For the two samples, recycled cardboard and rice, which are considered less complex due to their composition (e.g. fat content and disturbances due to matrix interference), the lowest laboratory comparison precisions were achieved. A significantly higher value for the reproducibility RSD_R was determined, as expected, for the MOAH fraction in the rice samples, whose concentration was within the laboratories' limits of quantification (approx. 0.5 mg/kg). This is the reason why MOAH is the parameter that can only be evaluated to a limited extent in this matrix.

In July 2017, the standard DIN EN 16955: 2017-08 "Foodstuffs - Vegetable oils and foodstuffs on the basis of vegetable oils – Determination of mineral oil saturated hydrocarbons (MOSH) and mineral oil aromatic hydrocarbons (MOAH) with online HPLC-GC-FID analysis" was published. Based on the international interlaboratory comparison test performed for the validation of the standard, for a MOSH level of 53.9 mg/kg, a reproducibility RSD_R of 23% and for a MOAH level of 50.7 mg/kg, a reproducibility of 31% can be expected. Within the laboratories, the expected repeatability is at least 1.5 times lower ($23\%/1.5 = 15\%$ or $31\%/1.5 = 21\%$). With coverage factor $k = 2$ the estimated measurement uncertainties U are between 30% and 40%, even for concentrations around 50 mg/kg.

A1.2 Limits of quantification

In table A2 below, typical limits of quantification (based on the results and experiences of the ILC participants) according to the current state of analysis are listed as orientation values in dependence on the fat content (Becker 2014). However, the limits of quantifications of the methods are not only dependent on the limitation of the separation columns for fat or oil, but also on numerous other factors, including the distribution of the detected hydrocarbons, interfering matrix components, additive enrichment methods and the chromatographic system used (column length, temperature programme, etc.).

Table A2: Possible limits of quantification of MOSH and MOAH dependent on the fat level of the food (Becker, 2014)

Fat content	Typical foods	Limit of quantification
< 4 %	Rice, corn, noodles	0.1 – 0.2 mg/kg
Up to approx. 20%	Cereals, muesli	0.5 mg/kg
Up to approx. 40%	Chocolate, nut-nougat paste	0.5 – 1 mg/kg
> 40 %	Vegetable oil	2 – 4 mg/kg

According to the comments of the standard DIN EN 16955: 2017-08 published in 2017, in terms of vegetable fat based food, the LC-GC coupling method is only suitable for MOSH and MOAH concentrations of more than 10 mg/kg each. The assessment was made based on the international interlaboratory comparison for the validation of this standard. In practice, for low levels the results from different laboratories may differ markedly. In any case, it must be ascertained that the contracted laboratories have the relevant expertise.

A1.3 Aspects critical for the evaluation

In the evaluation of the results of the interlaboratory comparison test (Becker, 2014), the following aspects were essentially classified as critical for analysis:

- Integration of chromatograms
- Base line
- Chromatographic cuts
- Chromatographic interferences

The comparison of the manual evaluation of the chromatograms in the respective laboratory with a standard, computer-aided evaluation showed that one of the main causes for deviating results is the different integration of the gas chromatograms. Basically, there are two different approaches: On the one hand, the „pragmatic“ approach, in which all peak signals on top of a mineral oil hump are not included in the sum of detected mineral oil hydrocarbons (MOH). It was this approach that was preferred by the majority of laboratories in the ILC test. On the other hand, if the peaks on top of the hump are not included, the results for the MOSH fraction, in particular, can be assumed to be lower. For the MOAH fraction, the risk of a relevant underestimation of the hydrocarbon fraction is significantly less.

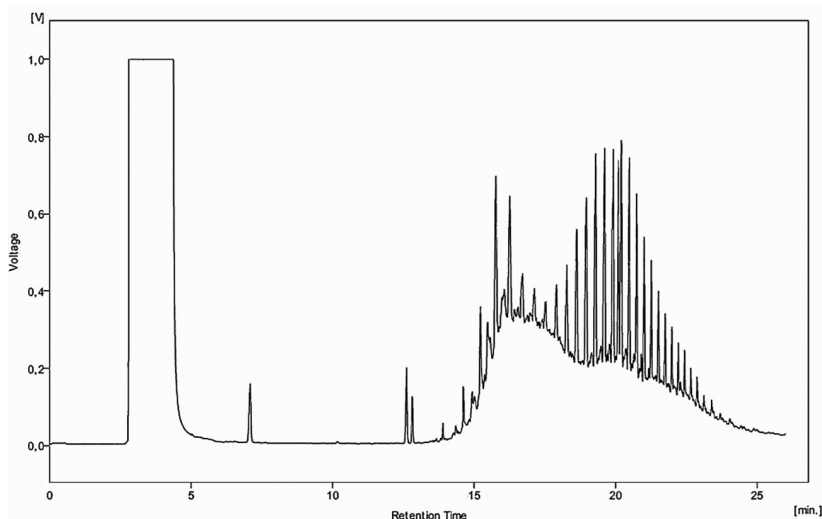


Figure A1: Example for peaks on top of the hump for a sample of recycled paper

Ultimately, it is a convention method that defines what is analytically determined as MOH. This approach is also preferred in the now available international standard (ISO/CD 17780).

A1.4 Test report requirements

In addition to the requirement of a standardized test procedure, it seems reasonable to specify details for evaluation in test reports for mineral oil analysis (e.g. integration with or without peak signals on top of the hump) in order to ensure comparability. It is essential to state the shape of the mineral oil hump. The mineral oil hump should be described in such a way so that this description can also be used in simplified calculation models for migration estimation.

This can be done in several ways as described below.

A1.4.1 Indication of the concentrations of the individual fractions

This can be done, for example, by specifying the different fractions in relation to the retention times of the *n*-alkanes (cf. DIN SPEC, 2018). The gas chromatographic retention time on a dimethylpolysiloxane phase of *n*-alkanes (e.g. $C_{10} - C_{40}$) is used for this purpose. Based on the retention times of the marker substances, time intervals (retention time ranges) are defined for both MOSH and MOAH, which serve as integration limits for the evaluation of the chromatograms.

The following integration intervals, for example, are frequently used:

- $C_{10} - C_{16} / C_{16} - C_{20} / C_{20} - C_{25} / C_{25} - C_{35}$
- $C_{16} - C_{25}$ (sum of substances that are mobile via the gas phase)
- $C_{16} - C_{35}$ (sum of all substances that are able to migrate)

Reproducibility of the absolute retention times must be ensured by regular measurement of an *n* alkane standard mixture. The integration of the *n*-alkanes and thus the determination of the absolute retention times of the C-numbers can take place at the beginning (rising slope), at the maximum of the signal (recommended!) or after complete elution of the marker alkane (baseline height). The C-number limits used for evaluation must be clearly documented (according to DIN SPEC 5010:2018-05) in the test report by stating the integration method used.

A1.4.2 Simplified method for describing the mineral oil hump

The AiF project has developed a simplified method that indicates the start, end and maxima of the mineral oil hump.

The description of the mineral oil hump without peaks on top can be simplified by indicating the start and end time and the maximum of the hump as well as the corresponding height of the peak. In order to describe double peaks and other irregular peak shapes, the description may additionally include the position of a second high point and the intermediate low point.

A1.4.3 Comparison of procedures using heavily contaminated recycled cardboard

In the following, the results stated for the concentrations of the individual fractions are compared with the described "simplified method for the description of the mineral oil hump". The sample used in this example is heavily contaminated recycled cardboard.

Table A3: Description based on fractions (recycled cardboard, MOSH)

Fractions	Peak area [mV min]
$C_{10} - C_{16}$	800.5
$C_{16} - C_{20}$	1154.5
$C_{20} - C_{25}$	706.4
$C_{25} - C_{35}$	829.5
$C_{10} - C_{35}$	3490.8
$C_{16} - C_{25}$	1961.7
$C_{16} - C_{35}$	2654.7

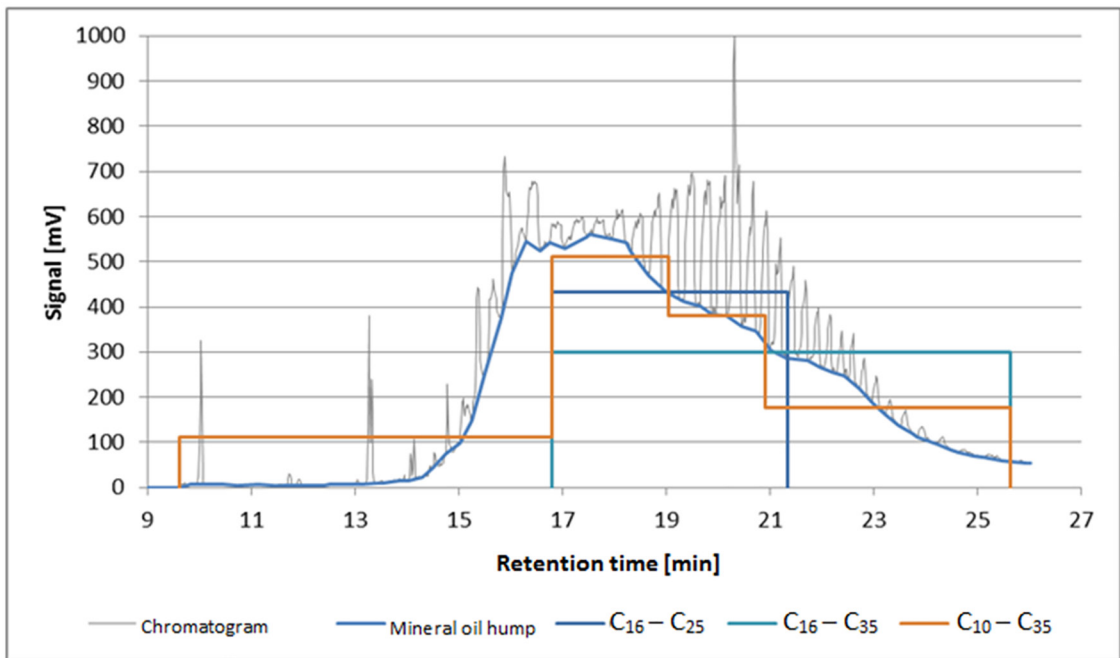


Figure A2: Description based on fractions (recycled cardboard, MOSH)

Table A4: Simplified description of the peak shape (recycled cardboard, MOSH)

	Retention time [min]	Signal [mV]
Start	14.02	14.28
Maximum	17.47	554.27
End	25.95	55.21

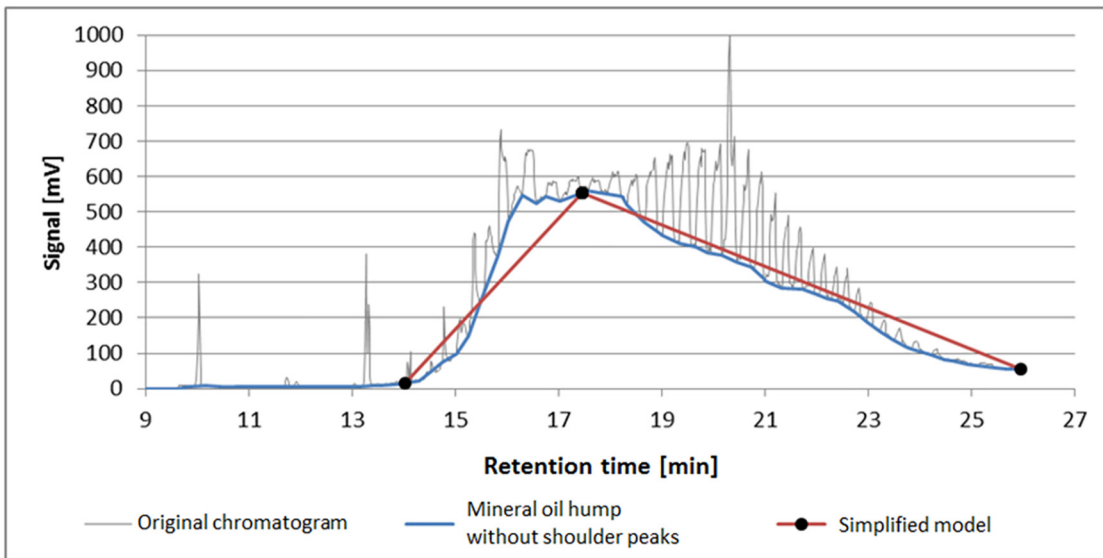


Figure A3: Example of a simplified description (recycled cardboard, MOSH)

Table A5: Comparison of integration results (recycled cardboard, MOSH)

Type of integration		Peak area [mV min]
With shoulder peaks		4164.8
Without shoulder peaks		3471.0
Simplified model	Calculated from mineral oil hump	3566.0
	Taken from chromatogram (relative to calculation)	3430.8 (96 %)

Table A6: MOAH – Description as fractions

Fractions	Peak area [mV min]
$C_{10} - C_{16}$	357.2
$C_{16} - C_{20}$	368.4
$C_{20} - C_{25}$	248.1
$C_{25} - C_{35}$	990.3
$C_{10} - C_{35}$	1964.0
$C_{16} - C_{25}$	691.8
$C_{16} - C_{35}$	1594.1

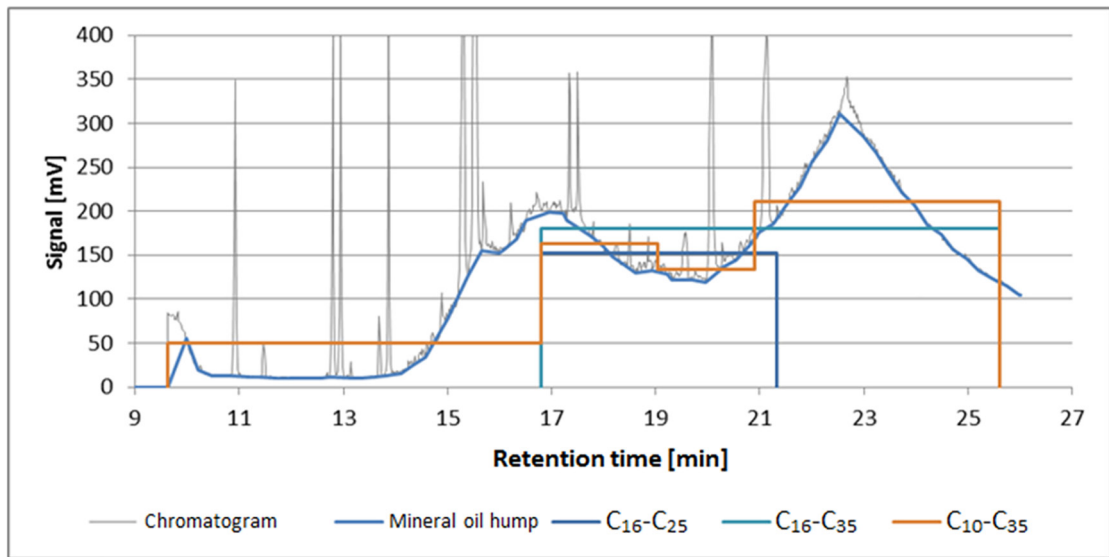


Figure A4: Description based on fractions (recycled cardboard, MOSH)

Table A7: Simplified description of the peak shape (recycled cardboard, MOSH)

	Retention time [min]	Signal [mV]
Start	14.10	15.46
Maximum 1	16.95	199.35
Minimum	19.97	119.59
Maximum 2	22.53	310.99
End	25.98	103.92

Table A8: Comparison of integration results (recycled cardboard, MOSH)

Type of integration		Peak area [mV min]
with shoulder peaks		2313.4
without shoulder peaks		2037.5
Simplified model	Calculated from mineral oil hump	2055.5
	Taken from chromatogram (relative to calculation)	2098.5 (102 %)

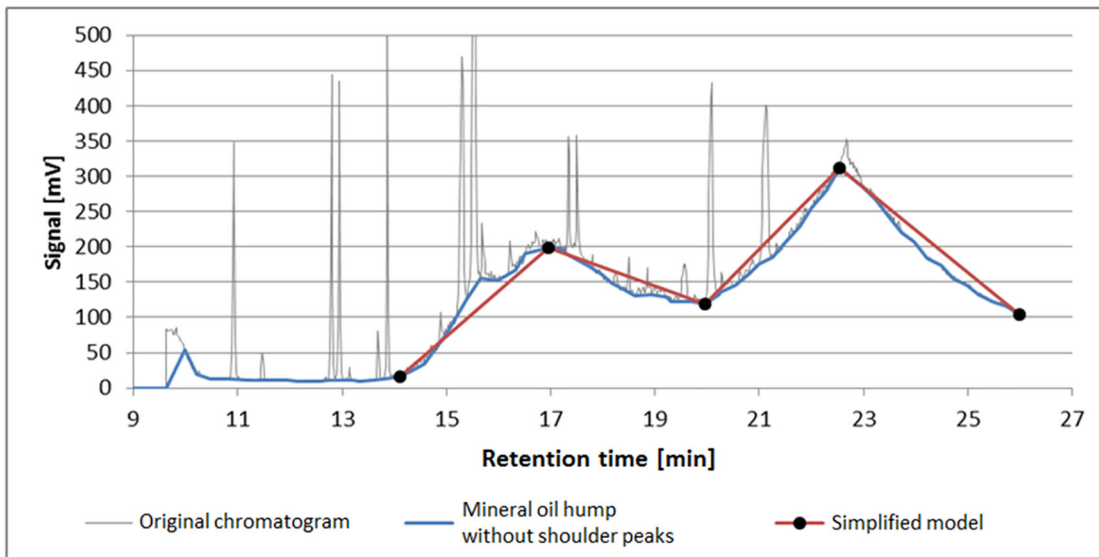


Figure A5: Description based on fractions (recycled cardboard, MOSH)

The comparison of the methods for the description of heavily contaminated recycled cardboard shows that both the specification of the concentrations of the individual fractions as well as the described „simplified method for the description of the mineral oil hump“ are sufficiently precise for the description of the mineral oil hump and for using it in simplified calculation models for migration estimation. When comparing the exact calculation from the original data using the “simplified method” with data taken from chromatograms, the deviations are clearly below 10%. Therefore, the “simplified method” can also be applied retrospectively for measurements for which, for example, only printed chromatograms and total values are available.

A1.4.4 Further requirements

There are some more important questions that need to be answered in a test report:

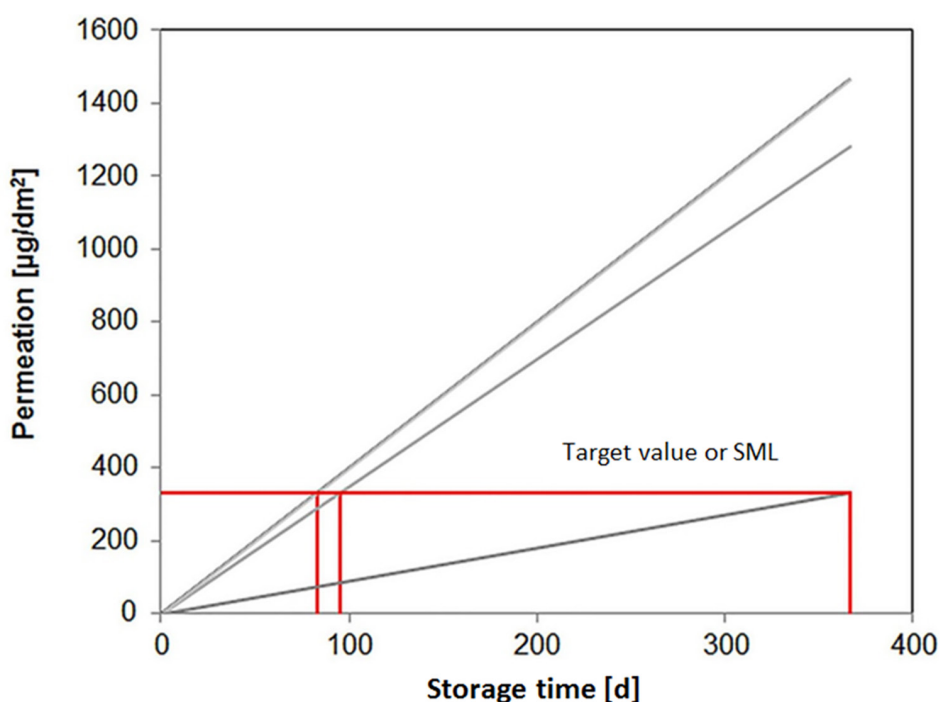
- Does the MOSH:MOAH ratio indicate the presence of fossil MOSH from crude oil? (Characteristically, the MOAH content in relation to the total MOSH content is between 15 and 35%).
- Do other substances, such as diisopropylnaphthalene (DIPN) present in recycled fibres, indicate migration from recycled fibres? (If no DIPN is present, recycled fibres can very likely be excluded as a source).
- Are there indicators for plastic-specific oligomers (e.g. POSH or PAO)?

In this regard, it should be noted that in the case of conspicuous positive results or for clarification of the interpretation of the results (e.g. identification of possible sources), it is recommended that the corresponding chromatograms are made available in addition to the analysis report.

A2 Evaluation methods for functional barriers

A simple evaluation method for a functional barrier is based on experimentally determined permeation rates. The use of cardboard spiked with model substances as a donor is a suitable option. The level should be around 750 mg/kg per substance (improvement of detection limits!).

The measured values of the experiments provide corresponding permeation rates for individual substances. Via the permeation rate, the time can be determined that is required to achieve the target values. As a worst-case approach, the permeation rate can be assumed to be constant from the start (lag time or permeation time is 0).



(Quelle: Fraunhofer IVV)

Figure A6: Worst-case assessment of the migrated amount of several model substances based on permeation rate and storage time

The permeation rates of the selected model substances also correlate approximately with their vapour pressure and thus also with the retention time of the substance on a (non-polar) GC column. This makes it possible to arrive at relatively accurate predictions about the amounts of migrating substances, even for complex substance mixtures. However, these model calculations based on experimental data must be prepared individually for each case.

A2.1 Permeation measuring techniques

The diffusion coefficient in the barrier layer is the material constant that is decisive for the evaluation of mineral oil barriers. The characteristics of a functional barrier may be determined with the following methods:

- Migration test (with LC-GC coupling)
- Permeation tests with static acceptor
- Permeation tests with dynamic acceptor
- Lag time experiments (provide diffusion and partition coefficient)

A2.1.2 Migrationstests (mit LC-GC-Kopplung)

In general, it is possible to determine the relative barrier properties by means of LC-GC coupling. Here again the use of model substances is recommended. For this method, functional barriers are placed between a donor (cardboard containing mineral oil or paper spiked with model substances) and an acceptor (simulant) and sealed against external influences (Figure A7).

The simulant Tenax® can be used as an acceptor as well. The determination of the relative barrier properties with this method is comparatively elaborate, since in contrast to the permeation measuring stand, only one measurement per batch can be carried out. One measuring cell thus corresponds to one measurement under certain parameters. This means that this methodology is also more susceptible to errors. The qualification of the amount of substance that permeated is carried out via LC-GC coupling.

However, this type of approach was proven successfully with sensitive barrier materials (e.g. biopolymers), which cannot be tested with the conventional measuring technique due to their defined conditions of use. One example is the required residual moisture of certain biopolymers (Guazzotti et al., 2015), which is difficult to maintain because of the continuous fumigation with nitrogen in the permeation measuring stand. Drying causes the functional barrier to crack and thus leak (Figure A8), whereas this effect does not occur in the process described here.

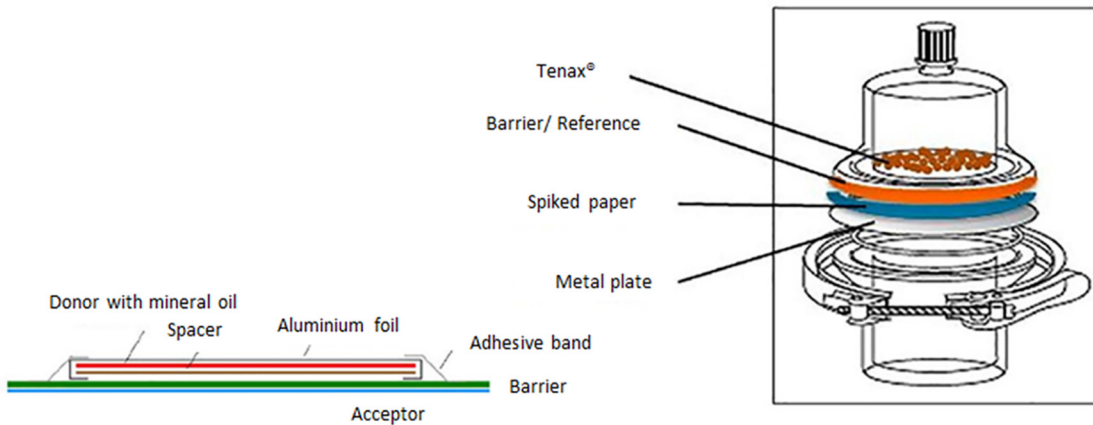


Figure A7: Examples for test layouts for the determination of relative barrier properties. On the left: Use of aluminium film (Source: K. Grob); on the right: Migration cell (Source: Fraunhofer IVV)

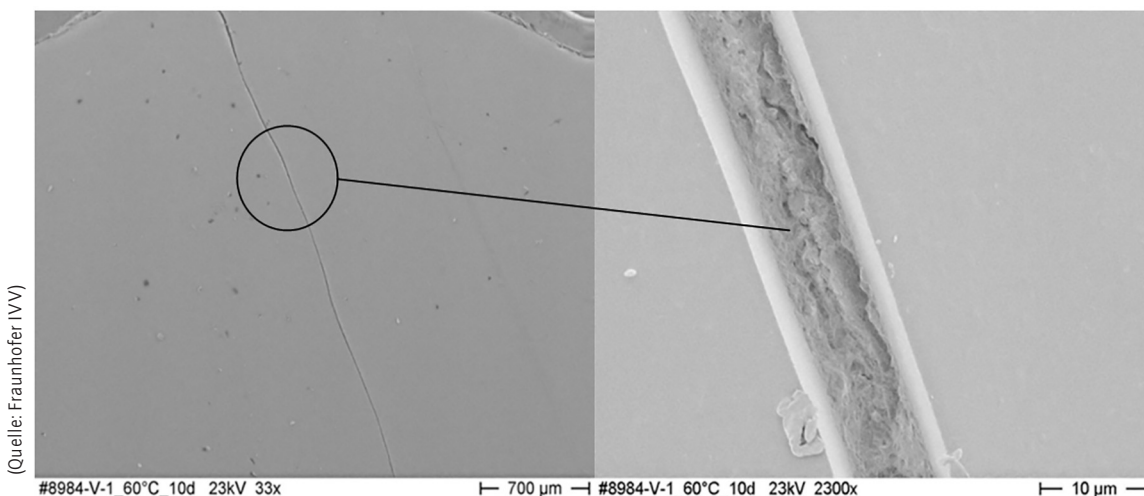


Figure A8: Brittle cracks in a functional biopolymer barrier caused by removal of moisture from the polymer layer

A2.1.3 SVI Guideline

The Swiss „SVI-Guideline 2015.01_Innenbeutel“ (Swiss Packaging Institute (SVI), 2016) of 2016 defines the minimum barrier efficiency of inner bags required to effectively reduce migration from recycled cardboard into food. As a food simulant, it uses a special silicone paper (paper with 20% dimethylpoly-siloxane), which may also be a suitable food simulant. The evaluation based on the SVI guideline applies only to the test conditions applied. However, the results can be converted to other temperatures using the Arrhenius equation. Since the results depend on the general conditions applied (concentration of the model substances, temperature, packaging area), this limits the significance of the evaluation of functional barriers and also makes comparisons between the results of different laboratories difficult (Ewender et al., 2016).

A2.1.4 Permeation tests

At Fraunhofer IVV, an automated measuring technique (at least one measuring point per day) was developed which allows the parallel determination of several films and forced tests (e.g. 40°C or 60°C) (Figure A9).

The material constants (diffusion and partition coefficients) obtained in the “lag time” experiment developed at Fraunhofer IVV allow the properties of a functional barrier to be comprehensively described by a computational evaluation (Ewender et al., 2013). For real packaging scenarios, the contamination of food with mineral oil components after a certain time can be predicted based on the initial conditions (e.g. initial concentration of the packaging, type of packaging, storage time and temperatures) (Ewender et al., 2016).

Layout IVV method

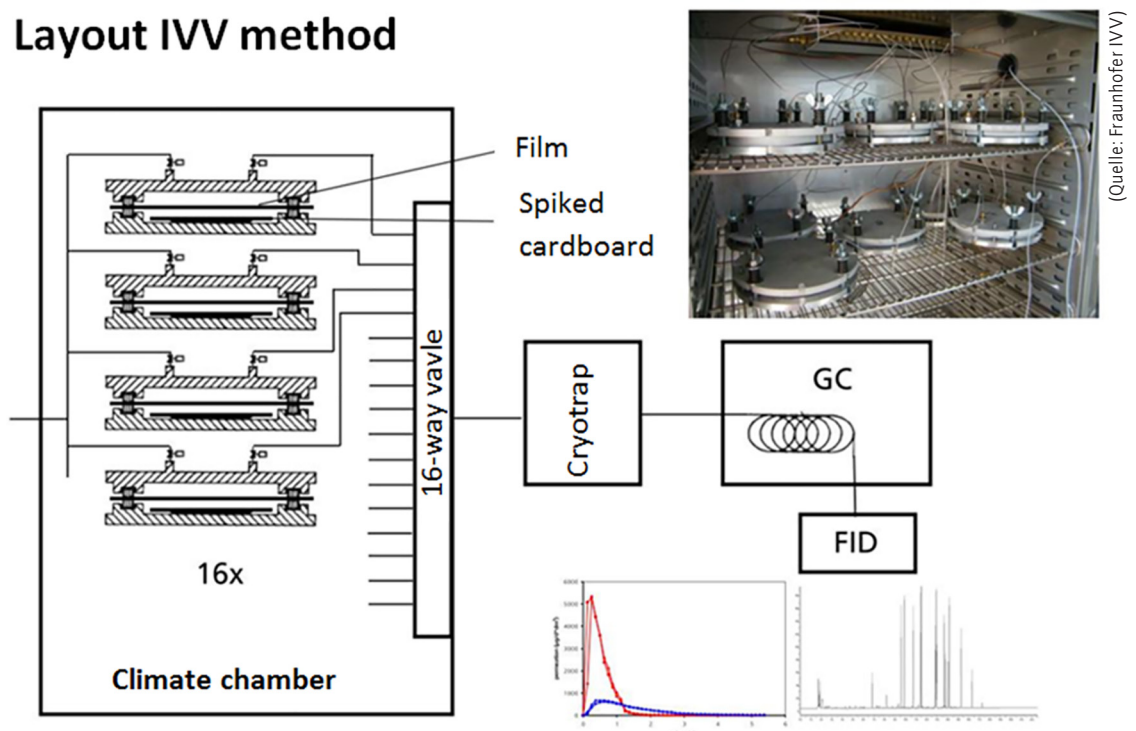


Figure A9: Permeation measurement with dynamic acceptor as a method for determining relative barrier properties

A2.1.5 Examples of permeation rates determined by experiment

The permeation rates determined are specific for the test conditions applied (e.g. temperature and initial concentration of the model components) and the structure of the test films.

Table A9: Experimentally determined permeation rate at 40°C for different model substances used (Ewender et al., 2015)

Compound	Model components for	Boiling point [°C]	Permeation rate [$\mu\text{g}/(\text{d dm}^2)$]					
			BOPP 20 μm	BOPP 20 μm , metallized	EVOH 20 μm	Acryl 31 μm	PVDC/Acryl 25 μm	BOPET 12 μm
Dodecane	MOSH	216	4900	1640	0.02	1.43	1.51	0.010
Naphthalene	MOAH	218	693	395	0.009	0.44	0.39	0.010
1-Methyl-naphthalene	MOAH	243	1590	808	<0.006	0.98	0.79	<0.006
Tetradecane	MOSH	254	1390	1250	0.014	3.90	4.05	0.008
1-Ethyl-naphthalene	MOAH	260	1000	690	<0.006	1.90	1.57	<0.006
2.7-Diisopropyl-naphthalene	MOAH	279	88.0	79.5	<0.006	1.30	1.45	<0.006
TXIB	Photo-initiators	280	244	103	<0.009	0.25	0.26	0.015
Hexadecane	MOSH	287	238	275	0.008	3.85	6.14	<0.006
Benzophenone	Photo-initiators	305	68.0	76.5	0.008	0.21	0.26	<0.007
Octadecane	MOSH	317	33.0	31.5	0.010	2.61	4.02	0.009
4-Methyl-benzophenone	Photo-initiators	326	22.0	22.5	0.017	1.27	0.59	0.017
Phenanthrene	MOAH	336	32.0	31.5	<0.006	1.37	1.00	<0.006
Eicosane	MOSH	343	5.51	4.95	<0.006	0.76	1.17	<0.006
Docosane	MOSH	369	1.02	0.90	<0.007	0.11	0.11	<0.007
Tetracosane	MOSH	391	<0.03	<0.03	<0.007	<0.007	<0.007	<0.007

A2.1.6 Performance of "lag time" experiments

The barrier materials are fastened inside in a permeation cell. In general, the measuring area is 191 cm². A large quantity of the permeants is filled into the lower part of the permeation cell. The upper part is constantly flushed with nitrogen. The permeated amount of substances is carried along with the stream of nitrogen and caught in an analytical trap. The complete quantity is then gaschromatographically desorbed and quantitatively measured. For the calibration, pure substance standards in known concentrations are used.

The example of a measured permeation curve of n-hexane at 40°C is shown in Figure A10. The actual measured value is the permeated quantity per area and time (lower graph). The cumulated measured values are then shown in the permeation curve (upper graph). The lag time is defined as the intercept of

the asymptote of the permeation curve. The diffusion coefficient D_p can be calculated from equation (A1) based on the lag time and the layer thickness l . Partition coefficient $K_{g/b}$ (g: gas, b: barrier) is calculated according to A2.

$$\text{lag time} = \frac{l^2}{6 \cdot D_p} \quad (\text{A1})$$

D_p : Diffusion coefficient
 l : Layer thickness

$$K_{g/b} = -\frac{A \cdot c_{\text{gas phase}} \cdot l}{6 \cdot \text{intercept}} \quad (\text{A2})$$

A: Contact area
intercept: Intercept of the asymptote

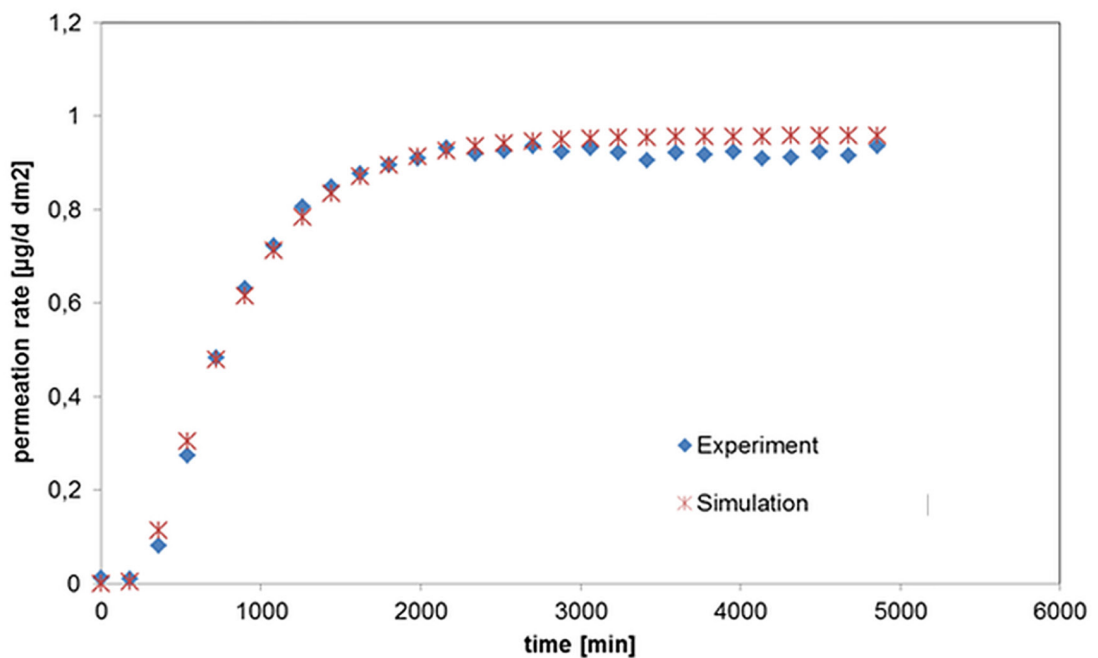
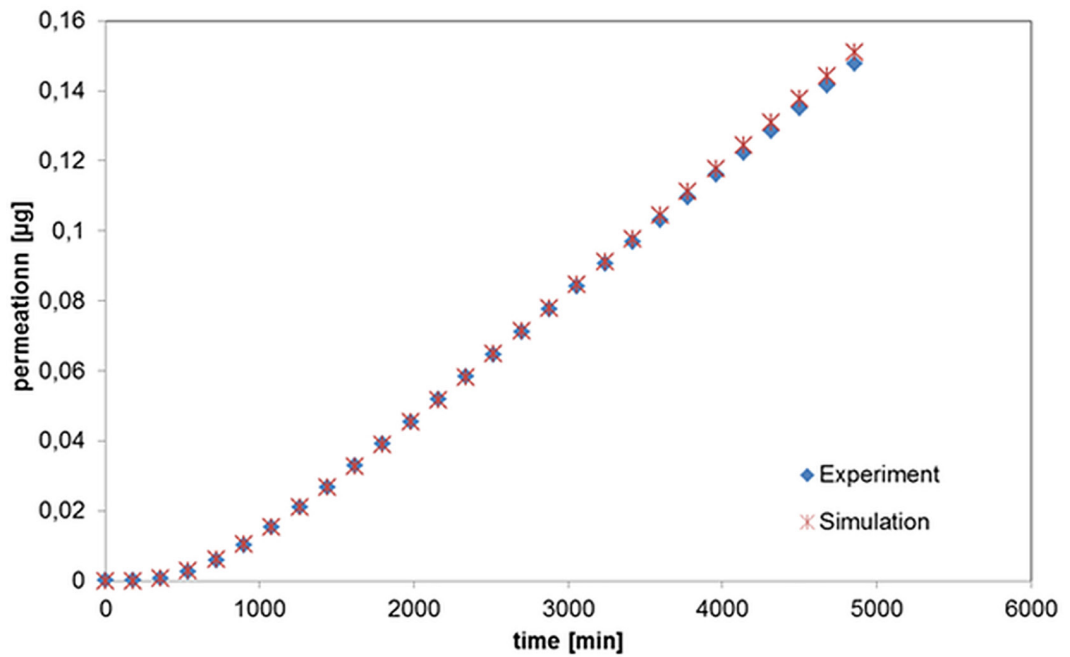


Figure A10: Experimentally determined permeation curve using an n-hexane sample at 40°C (upper graph: lag time curve, lower graph: permeation rate, blue dots: measured values, red dots: simulation) Simulation)

A2.1.7 Examples of data determined in lag time experiments

The results of a sample (EPOTAL® 8835 X coating to 40 µm BOPP) are exemplarily shown.

The diffusion coefficients from the measurements and the partition coefficients are summarized in the following tables.

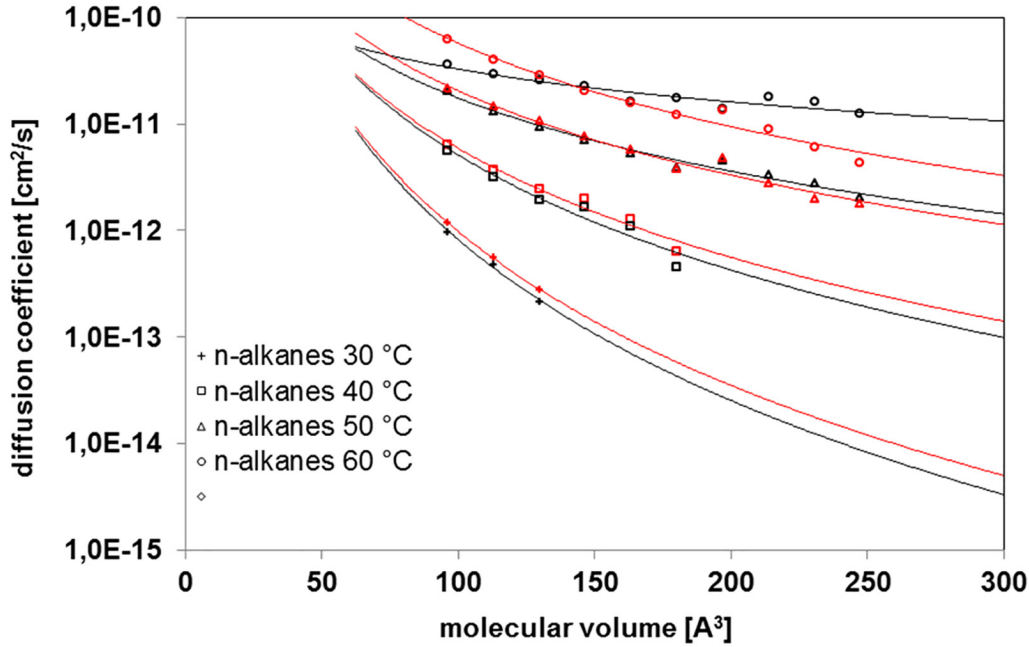


Figure A11: Correlation between molecule volume and diffusion coefficient for a sample

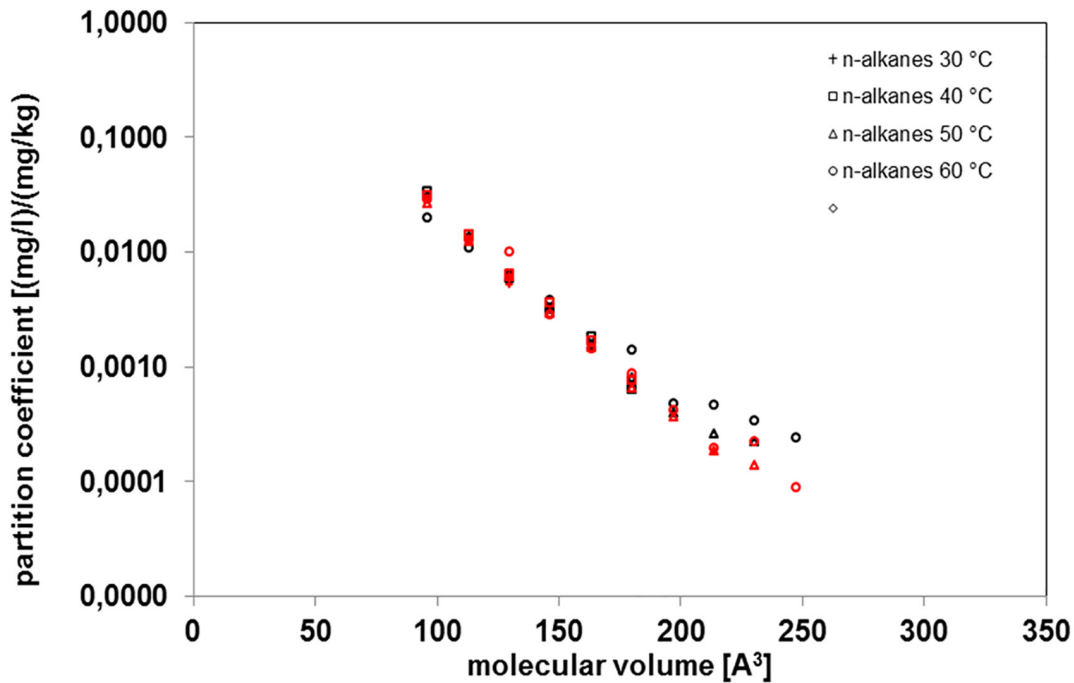


Figure A12: Correlation between molecule volume and partition coefficient for a sample

Table A10: Examples for diffusion coefficients determined experimentally from the lag time

Substance	Diffusion coefficient [cm ² /s] BOPP carrier to spiked gas stream				Diffusion coefficient [cm ² /s] Barrier to spiked gas stream			
	60 °C	50 °C	40 °C	30 °C	60 °C	50 °C	40 °C	30 °C
n-C ₅	3.66 10 ⁻¹¹	2.07 10 ⁻¹¹	5.57 10 ⁻¹²	9.73 10 ⁻¹³	6.28 10 ⁻¹¹	2.15 10 ⁻¹¹	6.41 10 ⁻¹²	1.18 10 ⁻¹²
n-C ₆	2.92 10 ⁻¹¹	1.33 10 ⁻¹¹	3.19 10 ⁻¹²	4.78 10 ⁻¹³	4.05 10 ⁻¹¹	1.48 10 ⁻¹¹	3.75 10 ⁻¹²	5.58 10 ⁻¹³
n-C ₇	2.57 10 ⁻¹¹	9.33 10 ⁻¹²	1.94 10 ⁻¹²	2.15 10 ⁻¹³	2.88 10 ⁻¹¹	1.08 10 ⁻¹¹	2.43 10 ⁻¹²	2.79 10 ⁻¹³
n-C ₈	2.92 10 ⁻¹¹	7.01 10 ⁻¹²	1.66 10 ⁻¹²		2.89 10 ⁻¹¹	7.67 10 ⁻¹²	1.99 10 ⁻¹²	
n-C ₉	1.61 10 ⁻¹¹	5.34 10 ⁻¹²	1.09 10 ⁻¹²		1.57 10 ⁻¹¹	5.75 10 ⁻¹²	1.27 10 ⁻¹²	
n-C ₁₀	1.74 10 ⁻¹¹	3.89 10 ⁻¹²	4.54 10 ⁻¹³		1.22 10 ⁻¹¹	3.78 10 ⁻¹²	6.31 10 ⁻¹³	
n-C ₁₁	1.39 10 ⁻¹¹	4.55 10 ⁻¹²			1.36 10 ⁻¹¹	4.78 10 ⁻¹²		
n-C ₁₂	1.79 10 ⁻¹¹	3.32 10 ⁻¹²			8.87 10 ⁻¹²	2.82 10 ⁻¹²		
n-C ₁₃	1.63 10 ⁻¹¹	2.80 10 ⁻¹²			6.06 10 ⁻¹²	1.99 10 ⁻¹²		
n-C ₁₄	1.14 10 ⁻¹¹	2.03 10 ⁻¹²			4.38 10 ⁻¹²	1.77 10 ⁻¹²		

The determined diffusion coefficients D_p and the partition coefficients between the gas phase and the barrier $K_{g/b}$ are material constants for a given barrier/permeant pair. In contrast to this, the permeation rates normally used are dependent on both the concentration of the permeant and the layer thickness of the barrier. Barrier properties of the materials at different layer thicknesses and at different temperatures can be calculated from the diffusion coefficients and the partition coefficients.

A.2.2 List of complete functional barriers

Without calculation and further experimental verification, it can be assumed, for example, that the following materials are complete functional barriers, subject to the condition that the material is not damaged (e.g. pinholes) during processing.

Table A11: Completely functional barriers

Construction	Basic polymer	Barrier material
36 µm O-PET corona treated	PET	PET
12 µm PET metallised ^{*)}	PET	Metallization
12 µm PET-SiOx 80 nm ^{*)}	PET	SiOx
12 µm PET-SiOx 50 nm Ormocer-Laquer ^{*)}	PET	SiOx / Ormocer
12 µm PET / SiOx ^{*)}	PET	SiOx
12 µm PET / AlOx / adhesive / 30 µm PP	PP	PET-AlOx
6 µm aluminium ^{*)}		Aluminium
6 µm aluminium ^{*)} / PE	PE	Aluminium
15 µm OPA ^{**)}	PA	PA
12 µm PET	PET	PET
12 µm PVDC coated transparent polyester film	PET	PVDC
PE / EVOH 3 µm / PE total 30 µm	PE	EVOH

^{*)} Only without pinholes or other damage.

^{**)} Only if there is no swelling in the presence of water.

A.2.3 Calculated "safe" thickness of polymers until permeation

Without calculation and further experimental verification, it can be assumed, for example, that, provided they have the required thickness, the following materials are complete functional barriers (Table A12).

Table A12: Functional barriers and their respective material thickness

Polymer	Time/ Temperature	Required thickness of the functional barrier based on molecule size [μm]		
		$C_8 - C_{17}$	$C_{18} - C_{35}$	$> C_{35}$
LDPE, PP atactic	10 d / 60 °C	no FB	no FB	7000
	10 d / 40 °C	no FB	8800	2640
	10 d / 20 °C	7000	3000	800
	2 h / 100 °C	no FB	10000	3240
HDPE	10 d / 60 °C	no FB	9000	3300
	10 d / 40 °C	8500	3000	960
	10 d / 20 °C	2280	800	280
	2 h / 100 °C	no FB	6400	1800
PP homopolymer/isotactic; PP-R (random copolymer)	10 d / 60 °C	no FB	4600	1400
	10 d / 40 °C	3900	1480	500
	10 d / 20 °C	1080	440	160
	2 h / 100 °C	8000	3000	900
PET, PBT, PEN	10 d / 60 °C	91	35	12
	10 d / 40 °C	31	14	4
	10 d / 20 °C	9	4	2
	2 h / 100 °C	61	23	7
PS	10 d / 60 °C	127	49	16
	10 d / 40 °C	46	18	6
	10 d / 20 °C	17	7	3
	2 h / 100 °C	65	26	8
SBS	10 d / 60 °C	no FB	no FB	4600
	10 d / 40 °C	no FB	5800	1750
	10 d / 20 °C	5000	1900	600
	2 h / 100 °C	no FB	7600	3300
PA 6 ^{*)}	10 d / 60 °C	210	82	25
	10 d / 40 °C	80	32	11
	10 d / 20 °C	26	11	4
	2 h / 100 °C	105	40	14
PA 6.6 ^{*)}	10 d / 60 °C	565	225	70
	10 d / 40 °C	220	65	26
	10 d / 20 °C	76	28	10
	2 h / 100 °C	300	120	36
PA 12 ^{*)}	10 d / 60 °C	810	300	91
	10 d / 40 °C	420	114	34
	10 d / 20 °C	100	44	13
	2 h / 100 °C	400	147	46
Hard PVC	10 d / 60 °C	127	49	16
	10 d / 40 °C	46	18	6
	10 d / 20 °C	17	7	3
	2 h / 100 °C	65	26	8

^{*)} not swollen (dry)
fb: functional barrier

A3 Migration test with food simulants

A3.1 Background

The use of simulant foods to test the migration behaviour of MOSH and MOAH into food is only possible with certain limitations. MOSH and MOAH are complex mixtures of substances; their analysis in food is very difficult because of the matrix components. For simplification, migration into food can be shown by simulant foods. According to some studies such as BfR, 2012, and Zurfluh et al., 2013, the common simulant Tenax® (MPPO) is considered to be less suitable for the simulation of mineral oil transport in food. However, test conditions of the PIM (Plastics Implementation Measure) were applied for the experiments, which are not easily transferable to the migration of mineral oil compounds and paper-based packaging materials. A prerequisite for the successful use of Tenax® is the selection of suitable test conditions. This coincides with other information such as in DIN SPEC 5010:2018-05 or Castle, 2014, van den Houwe et al., 2018.

In tests conducted by the Fraunhofer IVV on the suitability of simulants, a novel rod-shaped adsorbent called SorbStar® was tested in addition to Tenax®, which is modified polyphenylene oxide powder with a large internal surface area. SorbStar® is a silicone-based, non-polar and ultrapure polymer (polydimethylsiloxane) with a small internal surface area, which because of its geometry adsorbs mineral oil compounds only via the gas phase.

A3.2 Test conditions

Suitable test conditions for the storage with Tenax® and SorbStar® are listed in the table below.

Table A13: Test conditions for the storage with Tenax® and SorbStar®

Time [Days]	Temperature [°C]	Evaluation of storage at room temperature
10	40	up to 12 months
30	40	up to 24 months

The conditions listed in the table are based on kinetic comparative studies between migration studies with Tenax® and real storage conditions. Test temperatures above 40°C for further acceleration of the process have proven unsuitable according to experience gained by Fraunhofer IVV and statements made by DIN SPEC 5010.

Table A14 lists the model substances used for simulating the migration of mineral oil into food.

Table A14: Model substances used for simulating the migration of mineral oil into food

Model substances MOSH:

n-alkanes from C₇ to C₄₀

Model substances MOAH:

2-Ethyl-naphthalene

Phenanthrene

1-Methylanthracene

1,3- Diphenylpropane

2,7- Diisopropyl-naphthalene

Triphenylene

1-Phenyldodecane

The selection of model substances was guided by several criteria. On the one hand, they should represent both MOSH and MOAH substances as best as possible. Accordingly, MOSH model substances should have a paraffin-like and, if possible, cyclic structure. MOAH model substances should be composed of one to four ring systems and contain alkylated side chains. On the other hand, the substances should have a broad volatility spectrum in order to cover the entire range of possible mineral oil contamination. Based on these criteria, other model substances can be selected.

Since in many packaging geometries the migration of substances into the food takes place only via gas phase (hydrocarbons up to molecule size C₂₅) and condensation on the food, SorbStar® can only adequately be used predominantly for tests at room temperature (Huber, 2014). In the event of direct contact between the packaging and the product and depending on the type of packaging material, the food and the packaging geometry, mineral oil components with higher boiling points may also migrate into the food. For this type of migration Tenax® is the simulant of choice.

Figures A13 and A14 show results of the simulated migration from spiked papers (alkanes as MOSH model substances) into Tenax®. A distinction is made between migration via direct contact and transport via the gas phase only. The tests were performed in migration cells. The percentages refer to the added quantity of the model substances.

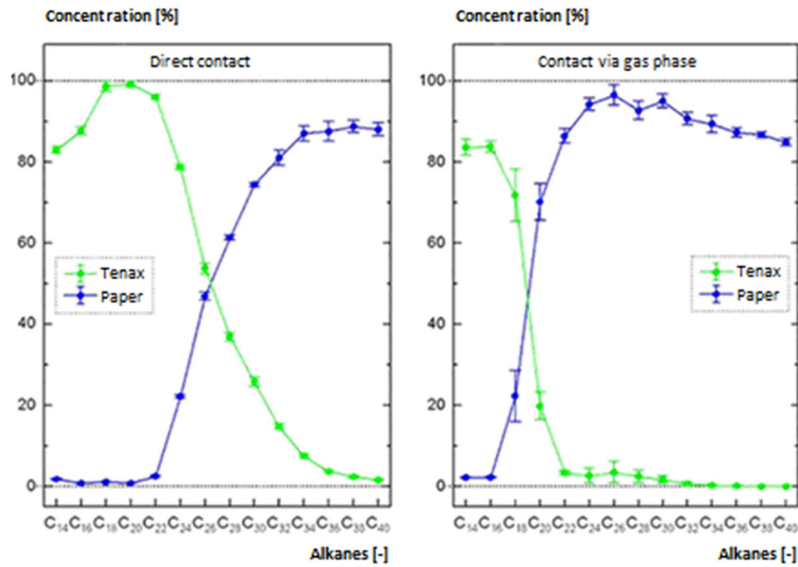


Figure A13: Alkane concentrations in Tenax® and paper after migration tests at 40°C for one day (left: direct contact, right: transport via gas phase)

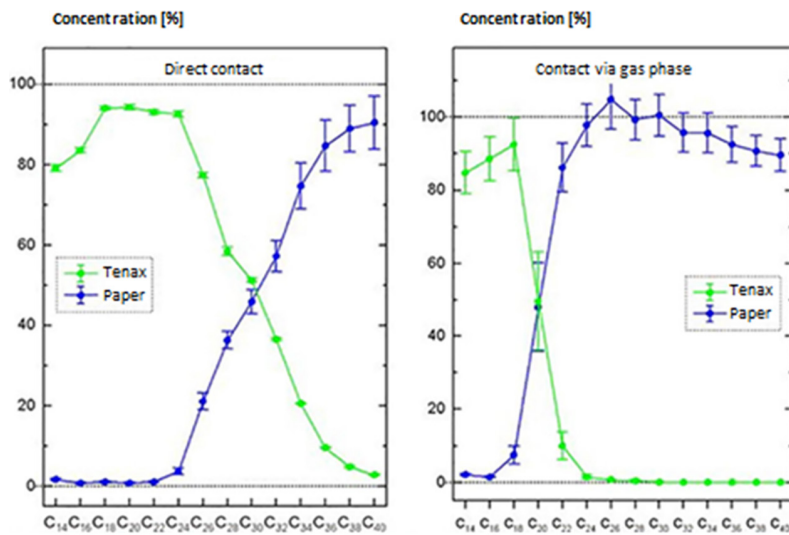


Figure A14: Alkane concentrations in Tenax® and paper after migration tests at 40°C for five days (left: direct contact, right: transport via gas phase)

It can be seen that migration via gas phase is largely restricted to molecules smaller than or equal to C_{24} , while in the case of direct contact between paper and simulant (corresponds to packaging and product), molecules up to C_{40} migrate. In the case of direct contact, a longer contact time increases the alkane concentration in Tenax®.

The choice of realistic conditions for migration tests is a prerequisite for obtaining meaningful values. Precise knowledge of the transport and storage conditions and times of the real food as well as the migration mechanisms is important. It should be taken into consideration that depending on the packaging geometry, migration can take place both via gas phase as well as via solid phase. However, in order to be able to assess this scenario more precisely, as a minimum requirement individual preliminary experiments with real packaging and food must be carried out. It is recommended that packaging spiked with model substances is used for this (see Table A14).

A4 Determination of partition coefficient $K_{p,f}$

A4.1 Background

Estimating the realistic partition coefficients via results of migration experiments is usually not precise enough because the amount of substances used for donor (paper) and acceptor (food) are usually too different and, especially in the case of fatty foods, fat or oil will migrate into the paper.

In order to achieve partition equilibrium between packaging and food, it is necessary to work at elevated temperatures. $K_{p,f}$ is calculated from equation (A3):

$$K_{p,f} = \frac{c_{p,\infty}}{c_{f,\infty}} \quad (\text{A3})$$

It can be assumed that partition coefficients are largely stable over a temperature range from 10°C to 45°C (Seiler & Franz, 2012). This is also confirmed by test results of permeation measurements already available (see A2.1.7).

A4.2 Test layout

For the determination of the partition coefficients between paper and food, the same weights of food that is not contaminated and paper or recycled cardboard spiked with model substances were stored for several days in a screw vial (40 ml ASE vial) in a heating cabinet at 60°C. Food samples were salt, rice, milk chocolate, marzipan and chopped hazelnuts. The recycled cardboard or the spiked paper was cut into approximately 6 x 15 cm strips that were rolled up and placed in the vial's neck above the food without direct contact. The storage periods were 3, 10 and 30 days.



Figure A15: Food (marzipan) and recycled cardboard in the vial; side view, closed vial (left) and top view, open vial (right)

At the end of the storage period, paper and food were extracted with n-hexane and analyzed with LC-GC. The partition coefficients were calculated from the ratio of the quantities of the individual fractions to the total quantities of paper and food used for the test.

A5 Numerical modelling of migrations

A5.1 Basic principles

The methods presented in the guideline for assessing the mineral oil migration from packaging materials to food include the total mass transfer method, which assumes the complete migration of contaminants into the food, and the equilibrium method, which assumes an equilibration between packaging and food. The equilibrium method represents the condition of a stationary system in which there are no more changes in the level of local contaminants. This final state results from dynamic diffusion processes through packing layers and the food and represents the end of the change in concentration in the observed system.

In this respect, the equilibrium concentration method represents a conservative simplification of migration processes, because the said equilibrium state may not be achieved before the end of the shelf life as the migration processes through packaging and food might be too slow. A dynamic, time-resolved diffusion model provides information on the development of contaminant levels in food.

For the modelling of diffusion processes, Fick's laws can be consulted, which allow a description of mass transport through packaging and food (Wang, et al., 2015 and Roduit, et al., 2005). Fick's diffusion law from a mathematical view can be described as being analogous to heat conduction; it is based on substance-specific parameters, which characterize the diffusion behaviour of different contaminants. Necessary parameters for the time-resolved description of diffusion are the diffusion coefficient (D), the partition coefficient (K) between packaging layers, the type of food, the initial concentration and the local distribution of contaminants (c).

The velocity of the mass transport is given by the material flow, which is defined by Fick's first law in equation (A4). The flux depends on the local concentration gradient, the diffusion area and the diffusion coefficient of the corresponding substance.

$$F = D\nabla c \quad (\text{A4})$$

F: Flux [$\text{mol m}^{-2} \text{s}^{-1}$]

D: Diffusion coefficient [$\text{m}^2 \text{s}^{-1}$]

c: Concentration [mol m^{-3}]

From Fick's second law, shown in equation (A5), results the change of the concentration over time in dependence of the local concentration gradient and the diffusion coefficient.

$$\frac{\partial c}{\partial t} = \nabla(D\nabla c) \quad (\text{A5})$$

Based on this modelling, composites of packaging materials and food products were simulated in order to be able to track a time-resolved change in the concentration in the food. Only in simple cases is it possible to solve the resulting system of partial differential equations analytically; therefore numerical methods must be used to solve the system. One approach to solve these systems is the Finite Element Method (FEM) or one of the Finite Difference Methods.

A5.2 Modelling of packaging material composites

When modelling packaging composites, they can be considered as successive layers in abstract form, characterized by their specific diffusion coefficients, the partition coefficients with respect to their adjacent layers and their layer thickness. Figure A16 shows a schematic representation. If the packaging layers are considered to be isotropic and internally homogeneous, the diffusion can be simplified and regarded as one-dimensional.

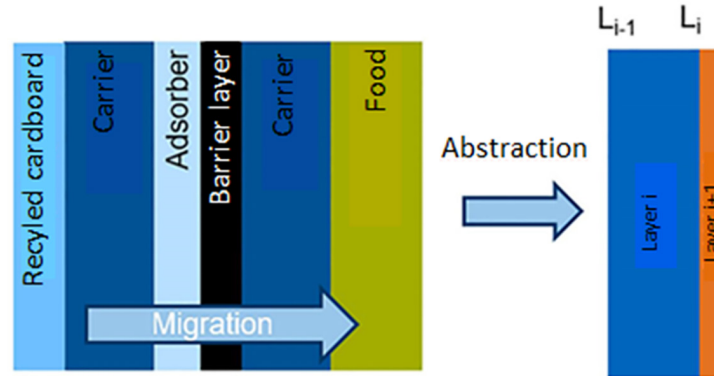


Figure A16: Representation of the n-layer migration model.

The material parameters for plastic composite films are often found in the literature. As an alternative, the diffusion coefficient can be determined in permeation experiments. In a so called lag time experiment, the time that a contaminant needs to permeate through a packaging material with a defined thickness is measured. The lag time can be determined by plotting the amount of migrated contaminant over time. The intersection of a straight line, which runs through the linear part of the permeation curve, with the abscissa marks the lag time. The diffusion coefficients can be calculated from the lag time as described in equation (A6) (Crank, 1975).

$$D = \frac{l^2}{6 \cdot t_{lag}} \quad (\text{A6})$$

l : Layer thickness [m]

t_{lag} : lag-time [s]

After all diffusion and partition coefficients are known, simulation of the packaging composite can be performed. The layers are lined up in the same order as they appear in the composite and the respective diffusion coefficients are allocated to the domains. For the FEM, the domains are divided into individual sub-elements (meshing), which are used to solve the systems of equations. For improved numerical stability, the elements at adjacent layer boundaries should be of similar size.

Migration from one layer into its adjacent layers is described by a continuity condition. This description ensures that there is no accumulation of contaminants at the phase boundary and that the adjacent layer absorbs exactly as much contaminant as was released by the original layer. For this, the layers are linked via their partition coefficients. The functional form of migration across the phase boundary is given in equation (A7). In addition, it may be necessary to consider the evaporation of volatile contaminants into the environment by defining a boundary layer condition.

$$F_{i+1} = K_{i,i+1} \cdot c_i - c_{i+1} \quad (\text{A7})$$

$K_{i,i+1}$: Partition coefficient

Such a model system allows simulating the time-resolved migration through the packaging layers into the food. An example for such a simulation is provided in Figure A17. Based on this basic simulation, it is possible to make a more detailed statement about the minimum shelf life, because migration kinetics has been taken into account.

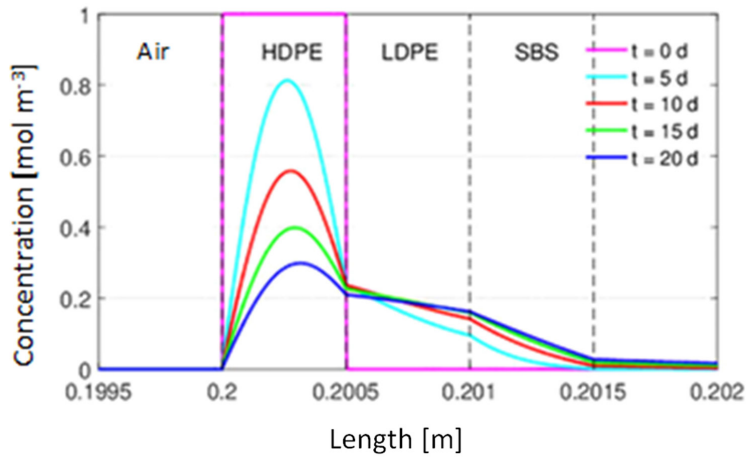


Figure A17: Time- and location-resolved simulation of a migration process through a packaging composite. On the left side of the HDPE layer, the contaminant is immediately removed by air.

In order to include storage at different temperatures into the model, an additional correlation of the diffusion coefficients with the storage temperature is necessary. As the partition coefficients are only to a lesser extent affected by temperature changes, their correlation with temperature was not included in the model in order to avoid additional complexity. In correlation with the temperature and the molecular weight of contaminants, Brandsch has developed an empirical equation, which has already been used in the past for the migration of petroleum components (Brandsch et al., 2002). Equation (A8) can be used to describe the effect of molecule size and temperature on the diffusion coefficient. The material parameter A_p is available from literature for many packaging materials.

$$D(T, M) = D_0 \cdot \exp\left(A_p - 0,1351 \cdot M^{\frac{2}{3}} + 0,003 \cdot M - \frac{10454}{T}\right) \quad (\text{A8})$$

- A_p : Material parameter [non-dimensional]
- D_0 : Reference diffusion coefficient [$\text{m}^2 \text{s}^{-1}$]
- M : Molecular weight [Da]
- T : Temperature [K]

Under the given assumptions of isotropic, homogeneous packaging layers, a modelling of the migration through the packaging is possible and has been validated on model systems. However, these assumptions do not generally apply to the food. Often the structure of food products is inhomogeneous and multi-phase. For instance, chocolate consists of a continuous fat phase in which cocoa and sugar particles are dispersed. These different phases have individual diffusion coefficients and partition coefficients amongst each other. Due to this mixture a calculation on the microscale using a structure similar to the food would be necessary. However, obtaining this structural information involves significant experimental effort and analytical equipment that may not be available.

For this reason the option is to express the mixtures via an effective diffusion coefficient that reflects the effect of the structure. If the diffusion coefficient of the food cannot be determined with sufficient accuracy, this will have a substantial effect on the remaining migration kinetics because an inaccurate local gradient is formed in the food, which influences the total kinetics. To calculate the migration of MOSH/MOAH, a tool was developed that depicts the permeation kinetics of MOSH/MOAH into food. Thus permeation kinetics is determined by the microscale of the food. A multi-scale approach is pursued: this means that effective material values are determined by calculations on the microscale.

A5.3 Determination of effective diffusion coefficients

The effective diffusion coefficients of the individual phases are required to predict the diffusion coefficients via the fine structure. One way to obtain an effective diffusion coefficient for a food is to subject the respective food to kinetic migration experiments. This involves the monitoring of the progress of the migration front, which emanates from a spiked carrier. Using Fick's law of diffusion and based on the concentration profile within the food, the parameters can be optimized. The aim of this optimization is to approximate a diffusion coefficient that best represents the experimentally observed values.

An experiment with cocoa butter cylinders stored on spiked cardboard as described below is an example for this procedure. The cylinders were divided into even layers along the direction of migration and the progress of the migration front was monitored. The results of the estimation of the diffusion coefficient are shown in Figure A18 as an example.

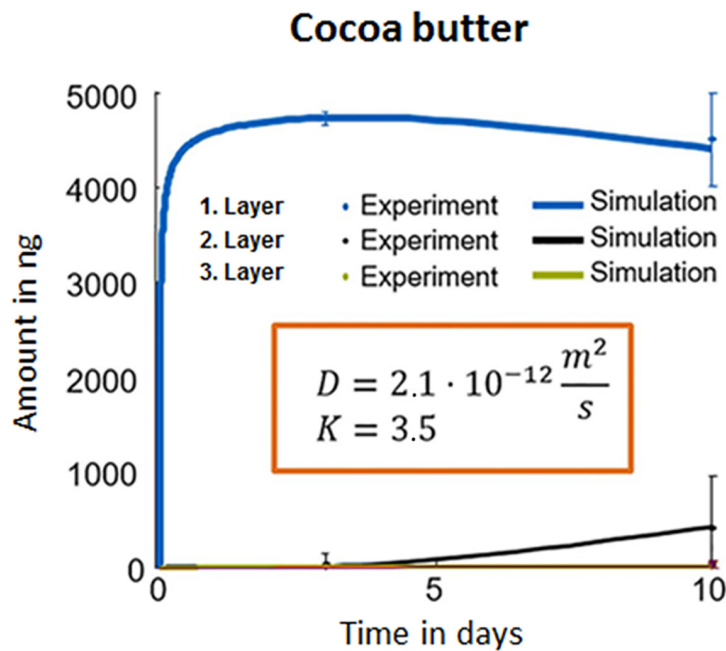


Figure A18: Concentration profile in a cocoa butter layer used to calculate the diffusion coefficient

This approach allows the estimation of diffusion coefficients based on migration experiments. In order to implement this approach into practice, essential analytical and experimental skills are still required.

For numerical calculation on the microscale, the fine structure is also determined by means of computer tomography measurements. Starting from this structure, similar artificial structures can be generated by software and the diffusion equation can be solved based on these structures in order to obtain an effective diffusion coefficient. This workflow is automated to perform the large number of calculations required for parameter variation. The result is the diffusion coefficient for similar structures but with different porosity or bubble diameter, for example.

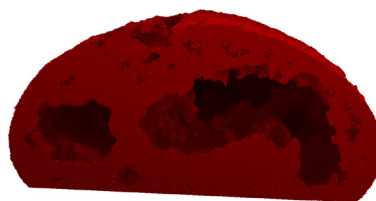


Figure A19: Cut through of a CT scan of an amaretto macaron

The effective diffusion coefficients calculated on the microscale cannot be described by literature models, as could be shown by comparing the models with simulated values. For some of the values, however, a model from the literature modified with an empirical correlation was able to produce good results. For the remaining data, a more powerful hybrid artificial neural network was designed and trained with data for spherical inclusions instead of the already presented approach using splines. The comparison of the effective diffusion coefficients simulated on the microscale with the diffusion coefficients calculated by fast correlations is shown below.

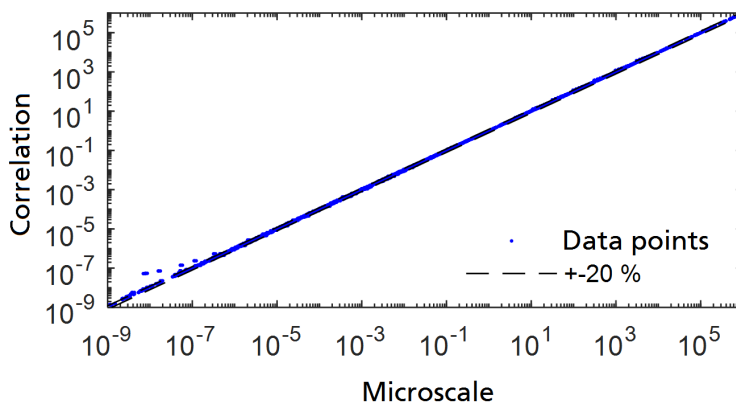


Figure A20: Effective diffusion coefficients calculated by correlation over the values obtained by simulation on the microscale.

A5.4 Outlook

The prediction of MOH migration based on fundamental experiments for individual food/packaging combinations is able to reduce necessary analytical investigations of producers to measurements of initial contamination and random checks of modelling results. By modelling the migration processes in food as well, the model achieves the highest possible significance and reliability. Appropriately selected tests with simulant foods are necessary in order to verify the results of the predictive models. The respective molecular mass distribution for MOSH and MOAH can be characterized by the retention times of the n-alkanes from the LC-GC chromatograms. The substance mixtures are then described in the model using "envelope curves" derived from the chromatograms.

Migration modelling, as introduced into European legislation for plastic packaging in 2001 as a new, alternative tool for compliance and quality assurance tests, can be beneficially applied in the field of MOH as shown. It allows the analysis efforts in businesses to be reduced while at the same time consumer protection is improved. The combination of mathematical simulation and experiments on the migration, permeation and adsorption behaviour of the compounds overrides analytical limits.

A6 Disclaimer

This guideline was developed by Fraunhofer IVV, Freising, and the Chair for System Process Engineering, TU Munich, Freising, within the framework of the IGF project "Measurement and prediction of the migration of mineral oil components (MOH) from packaging into food as a contribution to minimizing contamination" (AiF 19016 N) under the sponsorship of The Research Association of the German Food Industry (FEI), Bonn, Germany. It was funded by the Federal Ministry of Economic Affairs and Energy on the basis of a resolution of the German Bundestag.

The following companies and associations were involved in the preparation of the guidelines:

ACTEGA Terra GmbH, Industriestraße 12, 31275 Lehrte, Germany

ADM Cocoa B.V., Koog aan de zaan, The Netherlands

Alfred Ritter GmbH & Co. KG Schokoladenfabrik, Alfred-Ritter-Straße 25, 71111 Waldenbuch, Germany

Amcor Flexibles Singen GmbH, Alusingenplatz 1, 78224 Singen, Germany

August Storck KG, Paulinenweg 12, 33790 Halle (Westfalen), Germany

Backaldrin Österreich GmbH, Kornspitzstraße 1, 4481 Asten/Austria

Bahlsen GmbH & Co. KG, Podbielskistraße 9-11, 30163 Hannover, Germany

BASF AG, Carl-Bosch-Straße 38, 67056 Ludwigshafen, Germany

Bund für Lebensmittelrecht und Lebensmittelkunde e. V. (BLL), Claire-Waldoff-Straße 7, 10117 Berlin, Germany

Bundesverband der Deutschen Süßwarenindustrie e. V. (BDSI), Schumannstr. 4-6, 53113 Bonn, Germany

Cargill Cocoa and Chocolate, Eenhoornweg 12, 1531 ME Wormer/The Netherlands

CAVONIC GmbH, Schelmenbühl 15, 78333 Stockach, Germany

Constantia Hueck Folien GmbH & Co KG, Pirkmühle 14-16, 92712 Pirk, Germany

Crespel & Deiters GmbH & Co. KG Weizenstärkefabrik, Groner Allee 78, 49479 Ibbenbüren, Germany

Deutscher Fruchthandelsverband e. V., Bergweg 6, 53225 Bonn, Germany

DMK Deutsches Milchkontor GmbH, Heidbergstrift 1, 17087 Altentreptow, Germany

Eisbär Eis GmbH, Eisbärstr. 1, 21641 Apensen, Germany

Fachverband Faltschachtel-Industrie e. V. (FFI), Kleine Hochstraße 8, 60313 Frankfurt, Germany

FPE – Flexible Packaging Europe – EAFA e. V., Am Bonneshof 5, 40474 Düsseldorf, Germany

GALAB Laboratories GmbH, Am Schleusengraben 7, 21029 Hamburg, Germany

GfU Gesellschaft für Umweltchemie Analytik – Begutachtung – Forschung mbH, Schwanthalerstr. 32, 80336 München, Germany

Gutena Nahrungsmittel GmbH, Über dem Dieterstedter Bache 10, 99510 Apolda, Germany

H. & J. Brüggem KG, Gertrudenstraße 15, 23568 Lübeck, Germany

Hubergroup Deutschland GmbH, Feldkirchener Str. 15, 85551 Kirchheim b. München, Germany

Huhtamaki Flexibles Packaging Germany GmbH & Co. KG, Heinrich-Nicolaus-Straße 6, 87674 Ronsberg, Germany

Industrievereinigung für Lebensmitteltechnologie und Verpackung e. V. (IVLV), Giggenhauser Str. 35, 85354 Freising, Germany

Infopoint - Kakao und mehr. Christa Schuster-Salas, Ricarda Huch Str. 42, 72760 Reutlingen, Germany

Intersnack Group GmbH & Co. KG, Peter-Müller-Straße 3, 40468 Düsseldorf, Germany

Josef Bernbacher & Sohn GmbH & Co. KG, Lise-Meitner-Str. 5, 85662 Hohenbrunn, Germany

Lebensmittelchemisches Institut (LCI) des Bundesverbandes der Dt. Süßwarenindustrie e. V., Adamsstr. 52-54, 51063 Köln, Germany

Lieken Brot- und Backwaren GmbH, Auf'm Halskamp 11, 49681 Garrel, Germany

Lindt & Sprüngli International AG, Seestraße 204, 8802 Kilchberg/Switzerland

Lindt & Sprüngli GmbH, Süsterfeldstraße 130, 52072 Aachen, Germany

Lubeca Lübecker Marzipan-Fabrik v. Minden & Bruhns GmbH & Co. KG, Albert-Einsteinstr. 64, 23617 Stockelsdorf, Germany

Ludwig Weinrich GmbH & Co. KG, Diebrocker Straße 17, 32051 Herford, Germany

Mayr-Melnhof Karton Gesellschaft m. b. H., Wannersdorf 80, 8130 Frohnleiten/Austria

Mestemacher GmbH, Am Anger 16, 33332 Gütersloh, Germany

Mineralölwirtschaftsverband e. V., Georgenstraße 25, 10117 Berlin, Germany

Mitteldt. Erfrischungsgetränke GmbH & Co.KG, Langendorfer Straße 23, 06667 Weißenfels, Germany

Moritz J. Weig GmbH & Co. KG, Polcherstraße 113, 56727 Mayen, Germany

Müller Service GmbH, Zollerstraße 7, 86850 Aretsried, Germany

Müller's Mühle GmbH, Am Stadthafen 42-50, 45881 Gelsenkirchen, Germany

Peter Kölln GmbH & Co. KGaA Köllnflockenwerke, Westerstr. 22-24, 25336 Elmshorn, Germany

Petro-Canada Europe Lubricants Ltd., Auf der Konn 12, 56753 Mertloch, Germany

Polifilm Extrusion GmbH, Köthener Straße 11, 06369 Südl. Anhalt, OT Weißandt-Göلزau, Germany

ROWE MINERALÖLWERK GmbH, Im Langgawaan 101, 67547 Worms, Germany

Schwermer Dietrich Stiel GmbH, Königsberger Straße 30, 86825 Bad Wörishofen, Germany

SIG Combibloc GmbH, Rurstraße 58, 52441 Linnich, Germany

SQTS – Swiss Quality Testing Service, Grünaustraße 23, 8953 Dietikon/Switzerland

Südzucker AG Mannheim/Ochsenfurt, Wormser Str. 11, 67283 Obrigheim/Pfalz, Germany

The Lorenz Bahlsen Snack-World, GmbH & Co KG Germany, Rathenaustrasse 54, 63263 Neu-Isenburg, Germany

Treofan Germany GmbH & Co. KG, Am Prime Parc 17, 65479 Raunheim, Germany

Unilever Holding Deutschland GmbH, Knorrstraße 1, 74074 Heilbronn, Germany

UNITI - Mineralöltechnologie GmbH, Jägerstraße 6, 10117 Berlin, Germany

Verband der deutschen Getreideverarbeiter und Stärkehersteller e. V. (VDGS), Knesebeckstraße 74, 10623 Berlin, Germany

Verband der ölsaatenverarbeitenden Industrie in Deutschland e. V. (OVID), Am Weidendamm 1A, 10117 Berlin, Germany

Verband Schmierstoff-Industrie e. V., Süderstraße 73 a , 20097 Hamburg, Germany

Verband Deutscher Großbäckereien e. V., In den Diken 33, 40472 Düsseldorf, Germany

Wirtschaftsverband Papierverarbeitung e. V. (WPV), Hilpertstraße 22, 64295 Darmstadt, Germany

Zentis GmbH & Co., Jülicher Str. 177, 52070 Aachen, Germany

